FILE

INTERNAL DOCUMENT 279

I.O.S.

REPORT PREPARED FOR THE MINISTRY OF AGRICULTURE, FISHERIES AND FOOD UNDER A CONTRACT TO STUDY WAVE/CURRENT INTERACTION

P.G. Collar, G. Griffiths and E.G. Pitt

NATURAL ENVIRONMENT RESEARCH COUNCIL

INSTITUTE OF OCEANOGRAPHIC SCIENCES

INSTITUTE OF OCEANOGRAPHIC SCIENCES

Wormley, Godalming,
Surrey GU8 5UB
(042-879-4141)

(Director: Dr. A. S. Laughton, FRS)

Bidston Observatory,
Birkenhead,
Merseyside L43 7RA
(051-653-8633)

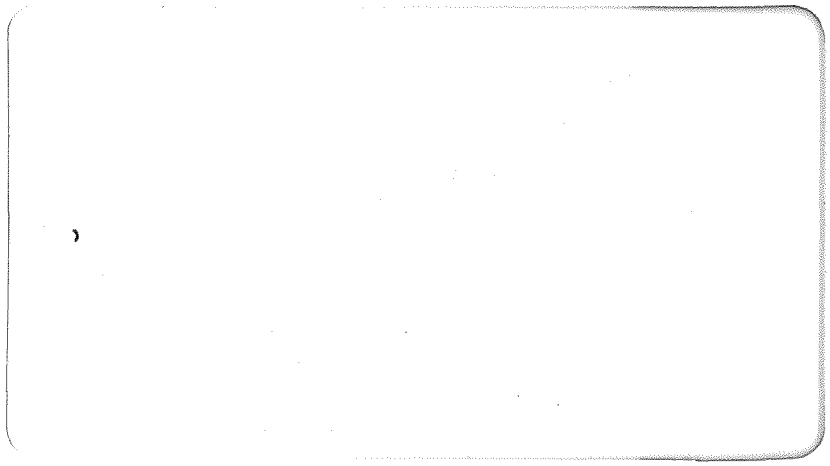

PG-36.

REPORT PREPARED FOR THE MINISTRY OF AGRICULTURE, FISHERIES AND FOOD UNDER A CONTRACT TO STUDY WAVE/CURRENT INTERACTION

P.G. Collar, G. Griffiths and E.G. Pitt

INTERNAL DOCUMENT NO. 279
1988

Institute of Oceanographic Sciences
Deacon Laboratory
Brook Road, Wormley
Godalming, Surrey
GU8 5UB

CONTENTS

LIST OF FIGURES

ABSTRACT AND CONCLUSIONS

The research reported on in this document includes three distinct yet related areas of work, involving measurements at two sites - off the East Coast and in the S.W. Approaches (figs. 1.1 and 1.2). Each may be regarded as an element in a continuing programme whose ultimate objective is to develop understanding of the way in which currents and current shears may modify the offshore surface wave field, and so provide a basis for improved techniques of offshore-inshore wave migration calculations. A further objective - to provide a reasonably detailed synoptic description of the offshore wave climate at Holderness (fig. 1.1), based on wave data collected by Waverider buoys - has been reported on separately.

At the outset it was not clear whether currents would greatly influence the directional properties of the surface wave field, and whether either vertical or horizontal shear would be important in this respect. The first two areas of work were therefore of an exploratory nature, attempting to establish the magnitude of any effect, and were essentially concerned with vertical shear. Measurements of horizontal shear would require an array of moored instruments - and hence considerably greater complexity - or possibly use of a remote technique which would enable currents to be mapped over an area. With the possible future direction of the work in mind the third area was focussed on this last possibility and took the form of a comparison between currents measured by h.f. radar and a moored instrument. This was thought to be relevant because previous comparisons had been made in areas of weak tidal currents and had shown some differences to exist between the two techniques: no surface comparisons had been done in strong tidal flows.

The areas of work were:-

1. To make a first order study of the effects of strong tidal currents on significant waveheight and mean wave direction at swell and higher wind wave frequencies, measured at a moored buoy; and to make complementary measurements at a site where tides were weak, but strong vertical shear might be expected.

2. Based partly on recent advances in instrument development at IOS, to investigate methods of measuring vertical current shear and to ascertain whether acoustic doppler techniques might be suitable for this purpose.

3. To investigate use of the h.f. radar technique for measuring surface currents in strong tidal flows.

SUMMARY OF CONCLUSIONS

Conclusions may be summarized as follows:-

1. A preliminary search for wave/current interaction effects on the commonly used parameters of the directional spectrum did not show any striking results. Doppler shifts were readily apparent, but effects on wave heights were not at all obvious. Further investigations should be carried out into effects on wave slope and spectral density.

2. Using specialized instrumentation and moorings high quality measurements were made of near-surface current profiles. Acoustic Doppler current profilers will have an important role in increasing the vertical resolution if suitable mooring methods can be developed for their deployment in the deeper areas of the continental shelf. The location of the site in the South-West Approaches, near the shelf break with strong stratification, gave rise to current shear from several sources, some of which would not be present closer to shore or in a well mixed region.

3. The comparisons made between OSCR and the moored buoy system at this site have, on the basis of some previous work (Collar and Howarth, 1987) in relatively weaker tidal streams, produced some unexpected findings. Previously, differences arose in strong wind conditions, and could be accounted for by differences in the way in which the two systems respond to vertical shear. Furthermore for one particular beam orientation there appeared to be some weak modulation of the tidal signal by the surface wave conditions. In the present set of data, obtained in conditions of strong tidal flow, and relatively lower windspeeds, measurements are well correlated but show, on occasion large tidally related differences, as well as a small mean bias. The similar systematic behaviour noted at the two OSCR stations is disturbing and should it be attributable to the OSCR measurement has implications for current mapping, particularly if residuals are of interest. Further investigation is clearly required.

1. INTRODUCTION

A better understanding of the interaction of waves and currents in conjunction with other research being sponsored by the Ministry in areas such as wave and surge forecast models and wave set-up will provide the tools for improved warnings of coastal flooding and improved design procedures for coastal protection works.

This report describes measurements of waves and currents made in the North Sea and in the South-West Approaches and discusses evidence for a number of wave/current interaction processes contained in the data.

Before proceeding, it may be helpful to make some general comments regarding the treatment of wave/current interaction in the literature.

There is a substantial literature on the interaction of waves and currents with reviews by Peregrine (1976), Peregrine and Jonsson (1983) and Srokosz (1985). While it is not appropriate to summarise these reviews at length the following general points should be noted. The available treatments consider three main aspects of the subject, and employ a rather different approach to each.

These aspects are:-

(a) A uniform train of waves on a depth-varying current and the resulting profile of water movement at a fixed position;

(b) Waves propagating on a current which varies with position, the aim being to predict changes in wave height, period and direction;

(c) Studies of the processes by which momentum from the wind/wave field enters the mean flow in the upper layers of the ocean.

The approach in (a) is to consider in detail the combination of a current of specified initial profile and a Stokes' wave expanded to high order to obtain the flow field in a series of regular waves (for discussion and references see Eastwood et al. (1987)). This approach is perhaps of more interest to designers of offshore installations than to coastal engineers.

The mathematical development in the subject as a whole is complex, but some simplification is possible in approach (b). In this, the exchange of momentum and energy between the current and the waves is formalised in terms of a "radiation stress" (Longuet-Higgins and Stewart, 1964), and can be summarised under the principle of the conservation of wave action (Bretherton and Garrett, 1968). Crapper (1987) gives a derivation of the conservation of wave action and various simple applications. Huang et al. (1972) use energy conservation to calculate the effect of a horizontally divergent current on the one-dimensional wave spectrum. From this and other analyses it is clear that the wave-field measured at one point depends on the generation and propagation history of the waves as they pass over the spatially varying current field. The effects of these interactions can be large: Gonzalez (1984) shows increases in waveheight of upto 100% in the Columbia River entrance.

The current measurements made in this project are essentially an approach (c) investigation with applications in the generation of ocean currents by wind and waves. These measurements are discussed in detail in Section 5, and summarised briefly below.

Near-surface currents were measured over a period of several weeks near the UKOOA databuoy, DB2, in the South West Approaches during the summer of 1986. A tidal analysis showed the presence of semi-diurnal shear caused by the non-linear interaction of the barotropic tide with an internal tide. During a storm with winds reaching 19 ms^{-1} the shear within the mixed layer was minimal, however, stronger shear developed during the after-response in the form of continental shelf waves and inertial oscillations. The measurement of the near-surface shear was examined in terms of the possible mix of Eulerian and Lagrangian components using a simple geometrical model.

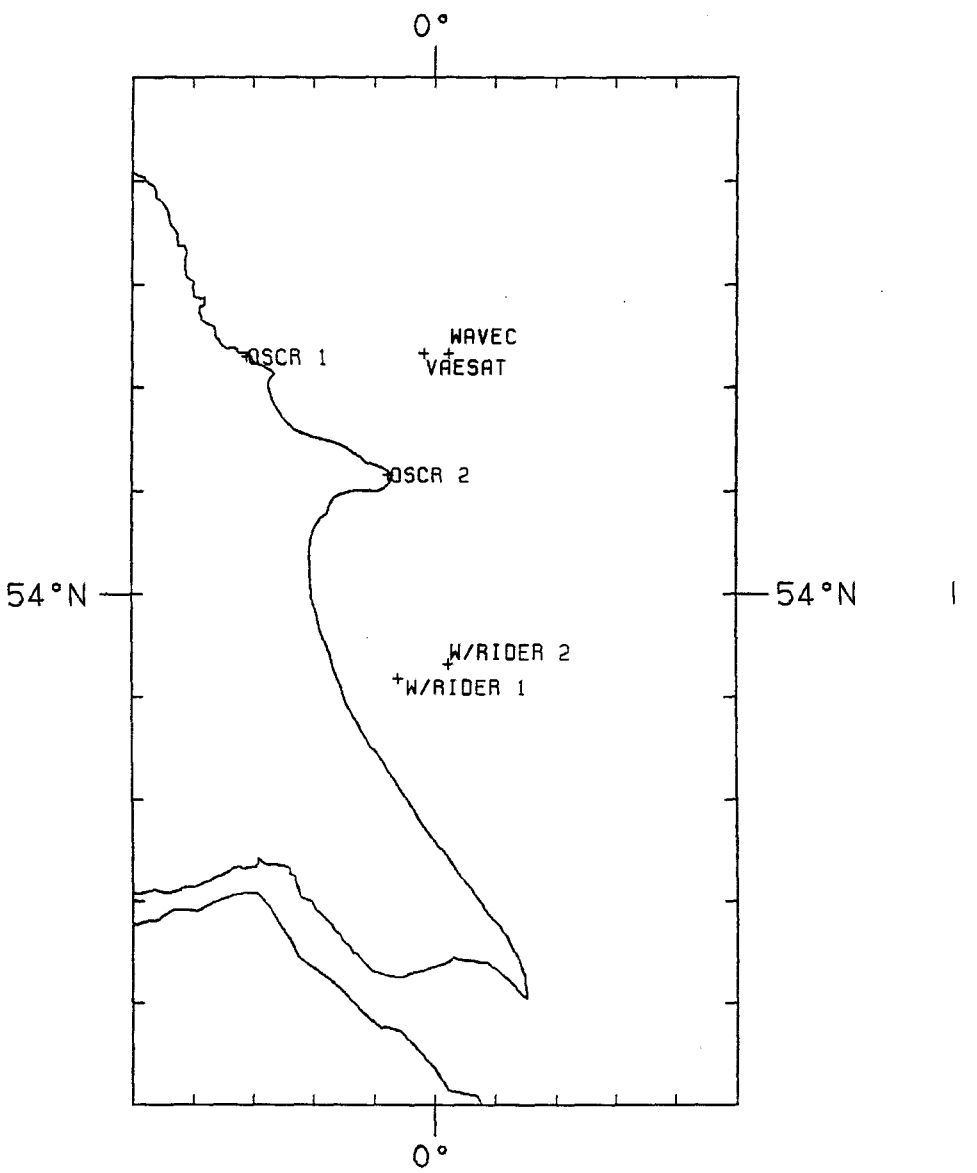

Figure 1.1 East Coast mooring sites and OSCR stations.

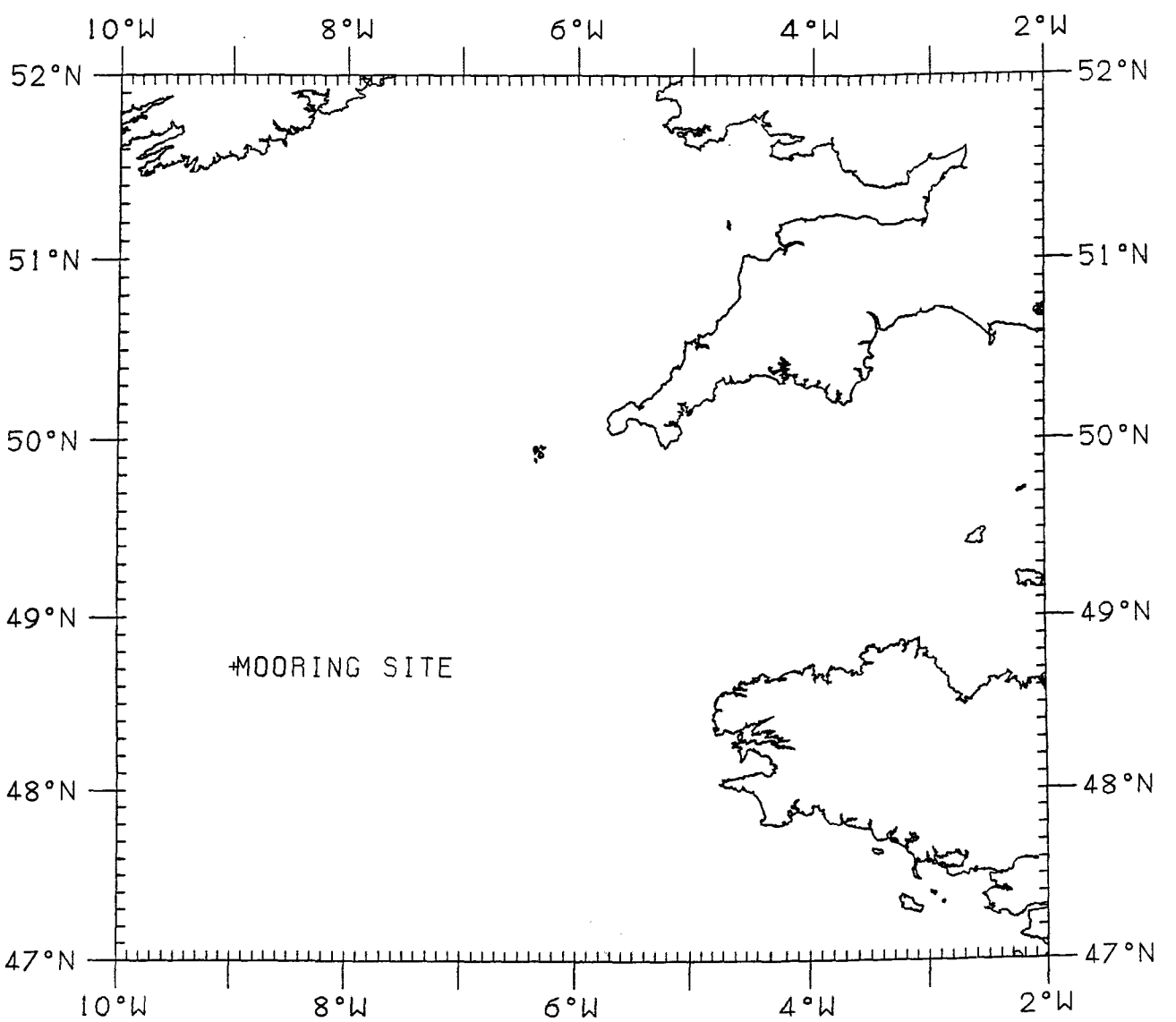

Figure 1.2 S.W. Approaches mooring site.

2. THE MEASUREMENT AND INTERPRETATION OF THE DIRECTIONAL WAVE DATA

The current measurements which were made in the North Sea off Flamborough Head are described in Section 4, and those made in the South-West Approaches are described in Section 5. In this section are described the wave measurements which were made at each site, and their interpretation.

2.1 Flamborough Head

Wave measurements were made using a Datawell Wavec pitch-roll buoy at 54°13.2'N, 0°1.8'E, i.e. about 7 miles NE of Flamborough Head in a depth of 50 m. (The buoy was deployed at the behest of the Department of Energy and the wave data from it, particularly for the period in March 1986 which is considered in this report, are commercially sensitive and may not be published).

The Wavec is a surface following buoy which is loosely moored to the sea bed by a compliant cable. The attachment of the mooring to the buoy is carefully designed so as to minimise the effects of mooring forces on the tilt response of the buoy. The basic measurements made by the buoy were the heave and the tilt of the buoy measured along two orthogonal axes. These along with the three components of the Earth's magnetic field and some housekeeping information were digitized at a rate of 1.28 Hz and telemetered to the shore station on Flamborough Head. Here, in addition to a number of checking functions, a receiver/microprocessor system performed the necessary calculations to give the 9 auto- and cross-spectral quantities which could be formed from series 1, 2 and 3 where:

1 = heave
2 = slope along the magnetic West axis
3 = slope along the magnetic North axis

i.e. C_{11}, C_{22}, C_{33}, the three autospectra and
C_{12}, Q_{12}, the co- and quad- spectra between heave and tilt West (magnetic)
C_{13}, Q_{13}, the co- and quad-spectra between heave and tilt North (magnetic)
C_{23}, Q_{23}, the co- and quad-spectra between slope West and slope North.

These were estimated at each of 64 frequencies from 0.0175 to 0.6375 Hz and written to magnetic tapes, which were sent to IOS Bidston (as it then was) at regular intervals. Here they were transferred to computer compatible magnetic tape. Further processing included transformations to refer the data to true North and East axes, and to convert the vertical measure to heave acceleration.

2.1.1 The derivation of directional parameters

The interpretation of the basic co- and quad-spectra followed the classical analysis of Longuet-Higgins et al. (1963) as reported by Pitt (1985). This analysis allows the evaluation of a number of 'parameters' of the directional spectrum at each frequency of the analysis.

We start by defining the directional spectrum of the variance of the waves:

If $S(f,\Theta)\ df d\Theta$ represents the variance of waves in the frequency band f to f + df and propagating from a direction interval Θ to $\Theta + d\Theta$, S is called the directional spectrum of the waves. The integral of the spectrum over direction gives the temporal spectrum, E, which would be measured by an omni-directional instrument like a wave staff or a Waverider buoy,

$$\text{i.e. } E(f) = \int_0^{2\pi} S(f,\Theta)\ d\Theta$$

A number of simple integral relationships exist between the co- and quad-spectra of the measurements and the directional spectrum, S. In particular we may evaluate the first five coefficients in the Fourier expansion of $S(f,\Theta)$, i.e.

$$a_n + jb_n = \frac{1}{\pi} \int_0^{2\pi} e^{jn\Theta}\ S(f,\Theta)\ d\Theta \qquad n = 1,2$$

$$a_0 = \frac{1}{2\pi} \int_0^{2\pi} S(f,\Theta) d\Theta$$

We note that $E = 2\pi a_0$; also in the following calculations it is convenient to

compute the normalised angular harmonics $A_n = a_n/a_o$; thus:

$$A_1 = \frac{Q_{12}}{\sqrt{C_{11}(C_{22} + C_{33})}}, \quad B_1 = \frac{Q_{13}}{\sqrt{C_{11}(C_{22} + C_{33})}}$$

$$A_2 = \frac{C_{22} - C_{33}}{C_{22} + C_{33}}, \quad B_2 = \frac{2C_{23}}{C_{22} + C_{33}}$$

where we have used the relation

$$\frac{C_{11}}{C_{22} + C_{33}} = \frac{(2\pi f)^2}{gk} = \tanh(kh)$$

(remember, series 1 is now vertical acceleration).

We suppose that the directional spectrum can be represented as the product of the temporal spectrum, E, and a spreading function, G, i.e.

$$S(f,\Theta) = E(f).G(f,\Theta),$$

and further we adopt a parametrical form for G:

$$G = \frac{1}{N(p)} .\cos^{2p}(\Theta - \Theta_1)/2,$$

where N is a normalising function which ensures that $\int_0^{2\pi} G(\Theta)d\Theta = 1$.

We may estimate the predominant or 'mean' direction Θ_1 at each frequency by $\Theta_1 = \tan^{-1}(B_1/A_1)$.

p, the spreading index, can be estimated from either the first or second harmonics, but it is now considered that the estimate from the second harmonic is less sensitive to noise, so

$$p = p_2 = \frac{1 + 3C_2 + \sqrt{1 + 14C_2 + C_2^2}}{2(1 - C_2)}$$

where $C^2_2 = A^2_2 + B^2_2$.

The angular spread can also be described by $\Theta_2 = \sqrt{2 - 2C_1}$, which for a narrow directional distribution approximates the r.m.s. angular half-width.

The 'check ratio' R is given by

$$R = \frac{1}{\tanh(kh)} \sqrt{\frac{C_{11}}{C_{22} + C_{33}}}$$

which should be unity for a perfect slope follower, so long as there is no current to disturb the normal dispersion relationship. If there is a current, the apparent frequency will be shifted; k, the value of the wavenumber calculated will be changed and will no longer agree with that inferred from the heave and tilt of the buoy. Thus R is modulated by tidal currents.

2.1.2 Parameters of the temporal spectrum

We define the moments of the temporal spectrum by $m_n = \int_{f_L}^{f_u} E(f) f^n df$. In practice the integral is replaced by a summation. We define H_s, the significant waveheight, by $H_s = 4\sqrt{m_0}$, T_z, the mean zero crossing period by $T_z = \sqrt{\frac{m_0}{m_2}}$ and T_1, the first moment period by $T_1 = \frac{m_0}{m_1}$. T_p is the reciprocal of the frequency at which the maximum value of E occurs.

2.1.3 Summary parameters

The directional spectrum even in its parameterised form contains a great deal of information. In order to reduce this to manageable proportions a summary of each observation was produced which contained the following:

H_s
T_z
T_1
T_p
Θ_1)
p) evaluated as average of three frequencies around the spectral peak
R)

H_s)
Θ_1) evaluated as average of six frequencies
p) at high frequencies
R)

The frequencies used in the evaluation of the moments and in the high frequency averages differed a little (for instrumental reasons) between the Flamborough and Southwest Approaches data sets and are tabulated below (in Hz):-

	moments		high frequency summary	
	f_L	f_u	hf_L	hf_u
Flamborough Head	.0075	.5975	.2575	.3075
South-West Approaches	.02875	.50875	.24875	.29875

2.2 South-West Approaches

Wave measurements were made by the large data buoy, DB2, which was moored in the South-West Approaches at 48°44'N, 8°50'W in a water depth of 156 m. The buoy is 6 m in diameter, and measures a range of meteorological variables as well as wave direction using the pitch and roll of the buoy. (The buoy was operated by Thorn E.M.I. Electronics Ltd on behalf of the United Kingdom Offshore Operators Association (UKOOA) Oceanographic Committee which is a consortium of oil companies and the Department of Energy. The data are commercial-in-confidence to this body, and while they may be used for the Ministry's purposes should not be published without UKOOA's permission).

The wave observations were made at 3-hourly intervals using a method similar in principle to that described for the Flamborough Head Wavec data, except that the vertical measurement was heave acceleration from the outset. Quality control checks and the processing into cross-spectra were carried out on board and the resulting data were recorded internally as well as being telemetered to shore via geostationary satellite.

The buoy was moored with a slack 3-point system, designed to provide high resistance to capsize combined with good surface following. Recent analyses of the system suggest that the tilt response is restrained by the moorings, and is moreover not axisymmetric. Since the degree and direction of the restraint changes according to wind, wave and current conditions, the directional data from the buoy are at present under question. Further study is underway on behalf of UKOOA to try to resolve these problems.

3. PRESENTATION OF THE DATA

The surface current and wind data for both data sets have been plotted along with the summary wave data defined above. Both sites are affected by tidal currents, although they are much stronger at Flamborough and without the complicating effects of stratification which are present in the South West Approaches data. The primary use of the wave data is to look for effects due to the passage of the waves across spatially varying and time varying current fields (approach (b) effects). Doppler shifts are the most obvious effect remarked on, but this is a first-order effect due to the bodily advection of the wave field by the current and the consequent change of wave frequency observed at a fixed point. Changes of height resulting from exchange of energy between the waves and currents are more difficult to substantiate and will require more detailed analysis.

3.1 Flamborough Head

A period in March 1986 was selected in which wave, wind and surface current data were available. This extended for 10 days from day number 71 to day number 80. So far it has only been possible to inspect these by eye for obvious signs of wave/current interaction. Some comments are given below.

Wind speed and direction, Figs. 3.1.3 and 3.1.2

The wind was mostly moderate from South or Southwest during the period, but with strong winds from the West around days 79 and 80.

Current Speed and Direction, Figs. 3.1.3 and 3.1.4

These are dominated by semidiurnal tidal currents, particularly early in the period during spring tides. The flow is aligned approximately 330°-150°. Later, from day 78 in neap tide conditions there is evidence of wind/wave driven components at the surface, the South-going stream on night 79/80 being much stronger than the adjacent return flows.

Hs and Tz, Figs. 3.1.5 and 3.1.6

Hs is highly correlated with the windspeed. The highest waves (~2.5 m) occur very near the time of highest wind speed, even though the direction did not give a long fetch (~30 km). There is no obvious tidal dependence in H_s, but this requires more detailed study.

While T_z shows an overall positive correlation with waveheight there is also a strong tidal dependence, suggesting Doppler shifting of the observed wave spectrum, - this effect should be examined more closely.

Peak Frequency, 1/Tp, Fig. 3.1.7

The spectral estimates have considerable statistical variability and the frequency of the spectral peak reflects this. The sequence of lower values on days 75-76 is associated with swell, the wind-wave peak having diminished below the level of the swell peak. There is some rather inconclusive evidence of Doppler shifting, and indeed one would expect the observed frequency of the spectral peak to be modulated in this way.

Mean Direction, Spectral Peak, Fig. 3.1.8

These tend to be loosely correlated with the wind direction, except for the swell period referred to above when they are almost 180° different. No obvious tidal dependence is evident, but further work is required to confirm this.

Spread Parameter, Spectral Peak, Fig. 3.1.9

This shows some correlation with periods of strengthening wind and increasing sea state, however the highest values (about 50) are attained during the swell period on days 75-76. Another maximum occurred during the high-wave period on day 79. Possible tidal dependence requires further study.

Check Ratio, Spectral Peak, Fig. 3.1.10

This shows a strong tidal dependence, as would be expected (see Sec. 2.1.1). The details of the variation are not straightforward however e.g. on day 72. The mean is approximately 1, suggesting good surface following by the Wavec buoy.

Mean Direction, High Frequency, Fig. 3.1.11

This shows good correlation with the wind direction except for a period during day 76 when the wind speed was low, 0-8 kn (0-4ms^{-1}). There is no obvious tidal dependence, but more detailed work is required to confirm this.

Spread Parameter, High Frequency, Fig. 3.1.12

Values of the spread parameter are generally low at high frequencies, indicating a wide directional spread of wave energy.

Check Ratio, High Frequency, Fig. 3.1.13

This shows a strong modulation at tidal frequencies, as expected. Once again the fairly symmetrical variation about unity suggests that the buoy is following the surface well.

H_S, High Frequency, Fig. 3.1.14

This shows some evidence of tidal modulation which should be examined further.

3.2 South-West Approaches

A period of 15 days was selected from the end of July and the beginning of August 1986, day number 210 to 224. During this period directional wave measurements were available from DB2 as well as wind speed and direction and there were surface currents from the IOS(DL) instrument. The data were plotted and some comments derived from a preliminary inspection follow.

Wind Speed and Direction, Figs. 3.2.1 and 3.2.2

There were two strong wind events, one around day 213/214 and one around 217/219. Winds reached 38 kn ($19ms^{-1}$) in the first event and 37 kn ($18.5ms^{-1}$) in the second. Directions were S'ly veering W'ly in both events.

Current Speed and Direction, Figs. 3.2.3 and 3.2.4

The current data were rather noisy and so 20 minute averages instead of 10 are plotted. The current regime is very complicated with inertial oscillations and shelf waves as well as semi-diurnal and other tidal components. The currents are discussed in Sec. 5.

H_S and T_Z, Figs. 3.2.5 and 3.2.6

H_S reached over 8 m during the first strong wind event on day 213, over 6 m on the second, day 218 and fell below 1 m only briefly on day 222.

The highest values of T_z occurred with the highest values of H_s, and overall they were moderately well correlated - except for a period around days 222-225 when a long period swell affected the site.

Peak frequency, 1/Tp, Fig. 3.2.7

The lowest values occurred during the strong wind event on days 213-4 (perhaps anomalously low) and day 218. The abrupt fall on day 222 signalled the arrival of the swell.

Mean Direction, Spectral Peak, Fig. 3.2.8

During the strong wind events, Θ_1 (peak) veered from SSE to W in a similar fashion to the wind. On a number of occasions, though, the spectral peak was associated with residual swell. The swell event of days 222-5 is seen to be NW'ly in direction.

Spread Parameter, Spectral Peak, Fig. 3.2.9

The irregular variation was punctuated by somewhat higher values associated with actively growing wind sea or with the NW'ly swell of day 222 et seq. when p_2 exceeded 60.

Check Ratio, Spectral Peak, Fig. 3.2.10

This shows strong tidal modulation, as expected. Note that the mean of about 1.5 suggests suppression of the tilt response, possibly by the mooring.

Mean Direction, High Frequency, Fig. 3.2.11

This shows good overall correlation with the wind direction.

Spread Parameter, High Frequency, Fig. 3.2.12

Generally low values, indicating a wide directional spread at high frequencies.

Check Ratio, High Frequency, Fig. 3.2.13

This shows tidal modulation about a mean of approximately 1.2.

H_s, High Frequency, Fig. 3.2.14

Irregular variation with possible tidal modulation.

Flamborough Head -1986

Fig. 3.1.1

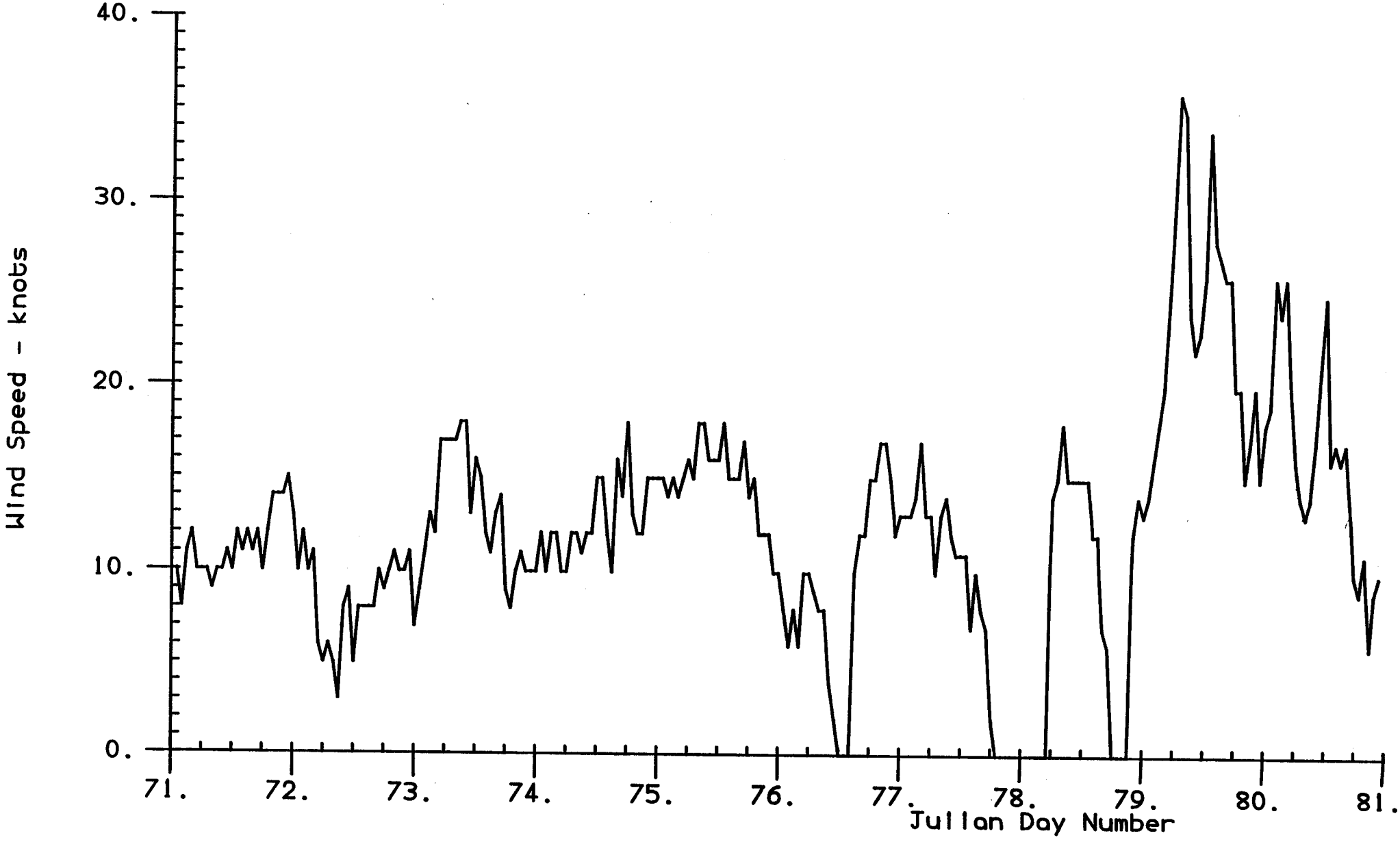

Flamborough Head -1986

Fig. 3.1.2

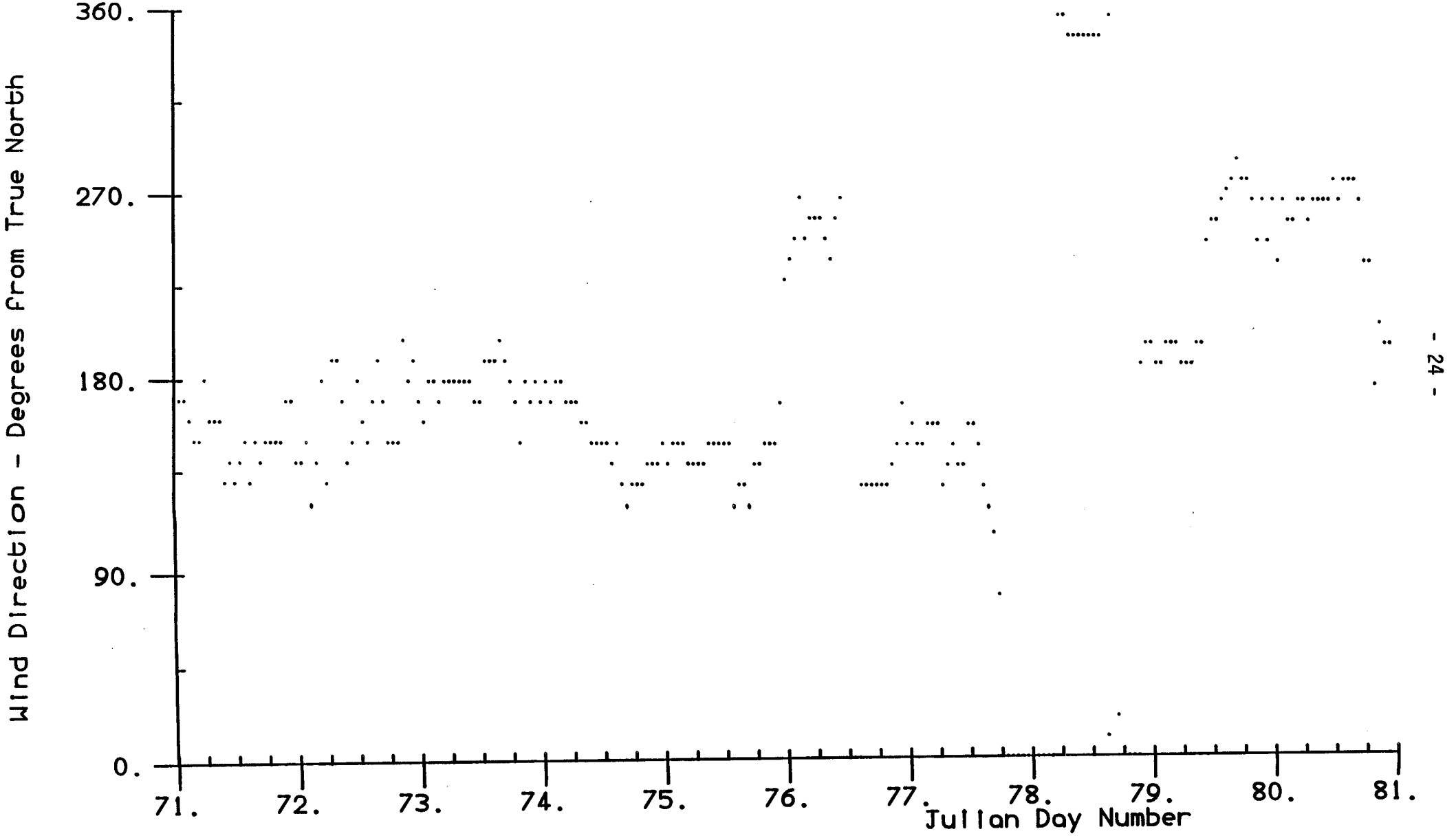

Flamborough Head -1986

Fig. 3.1.3

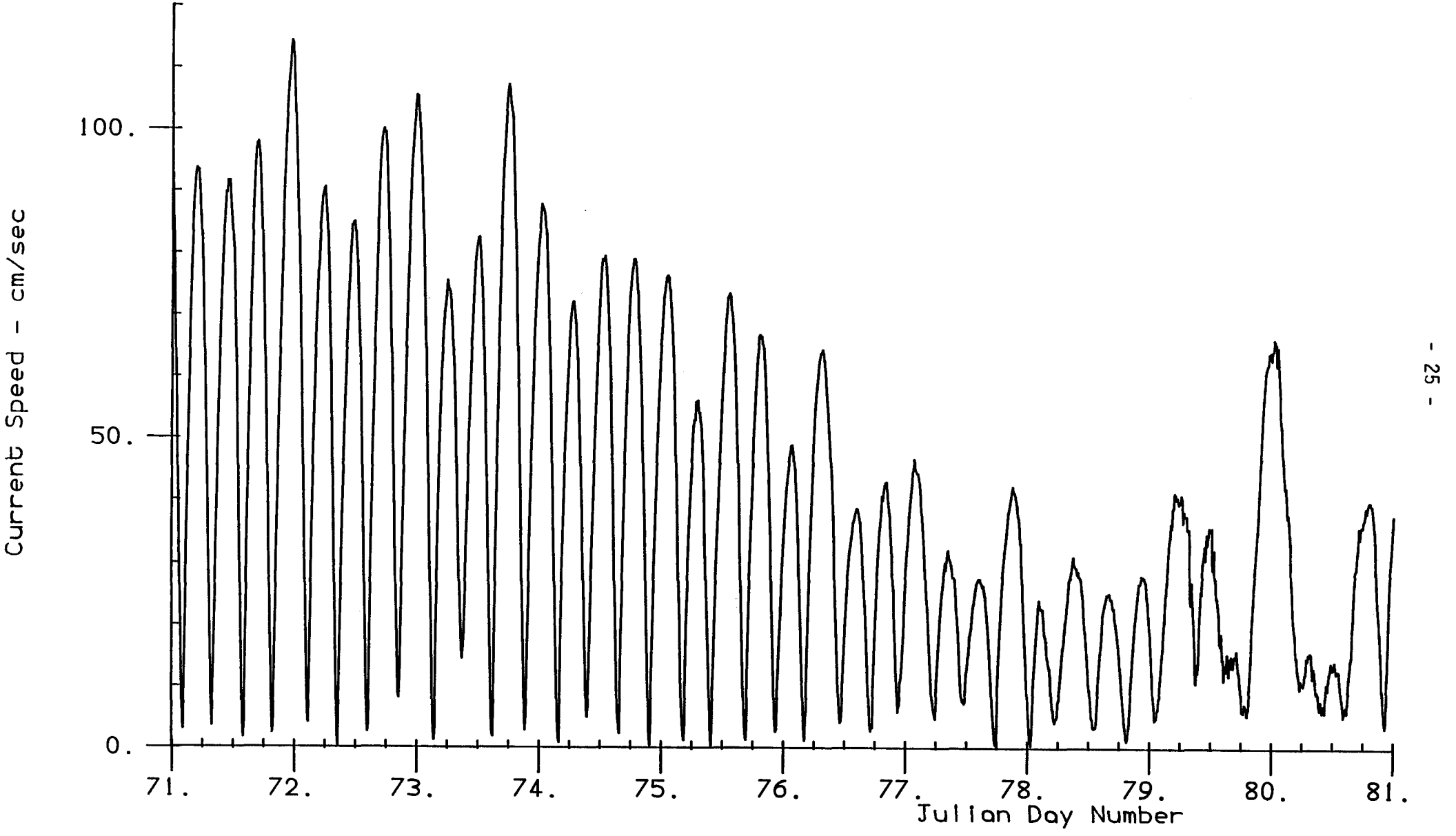

Flamborough Head -1986

Fig.3.1.4.

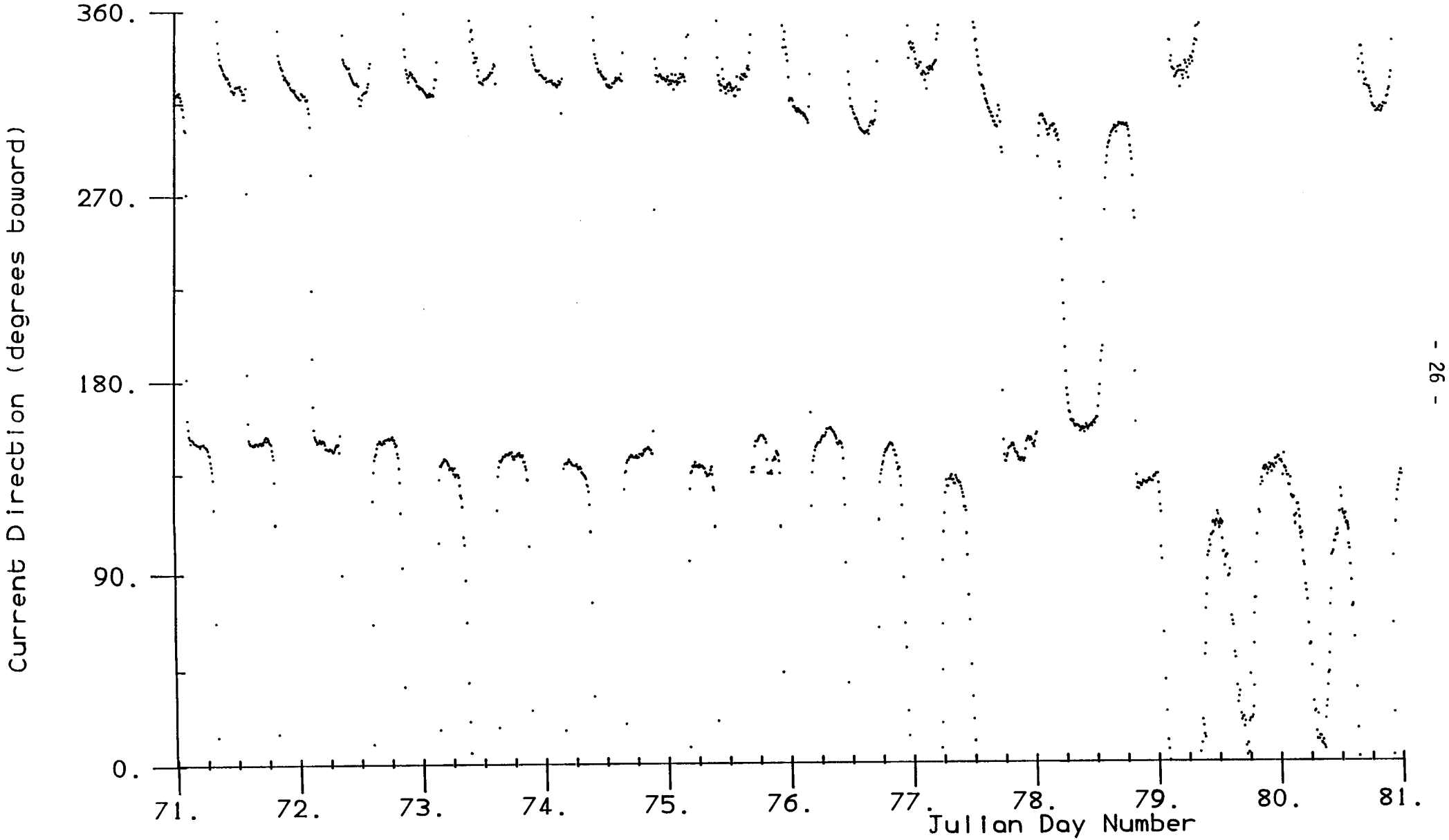

Flamborough Head - 1986

Fig. 3.1.5

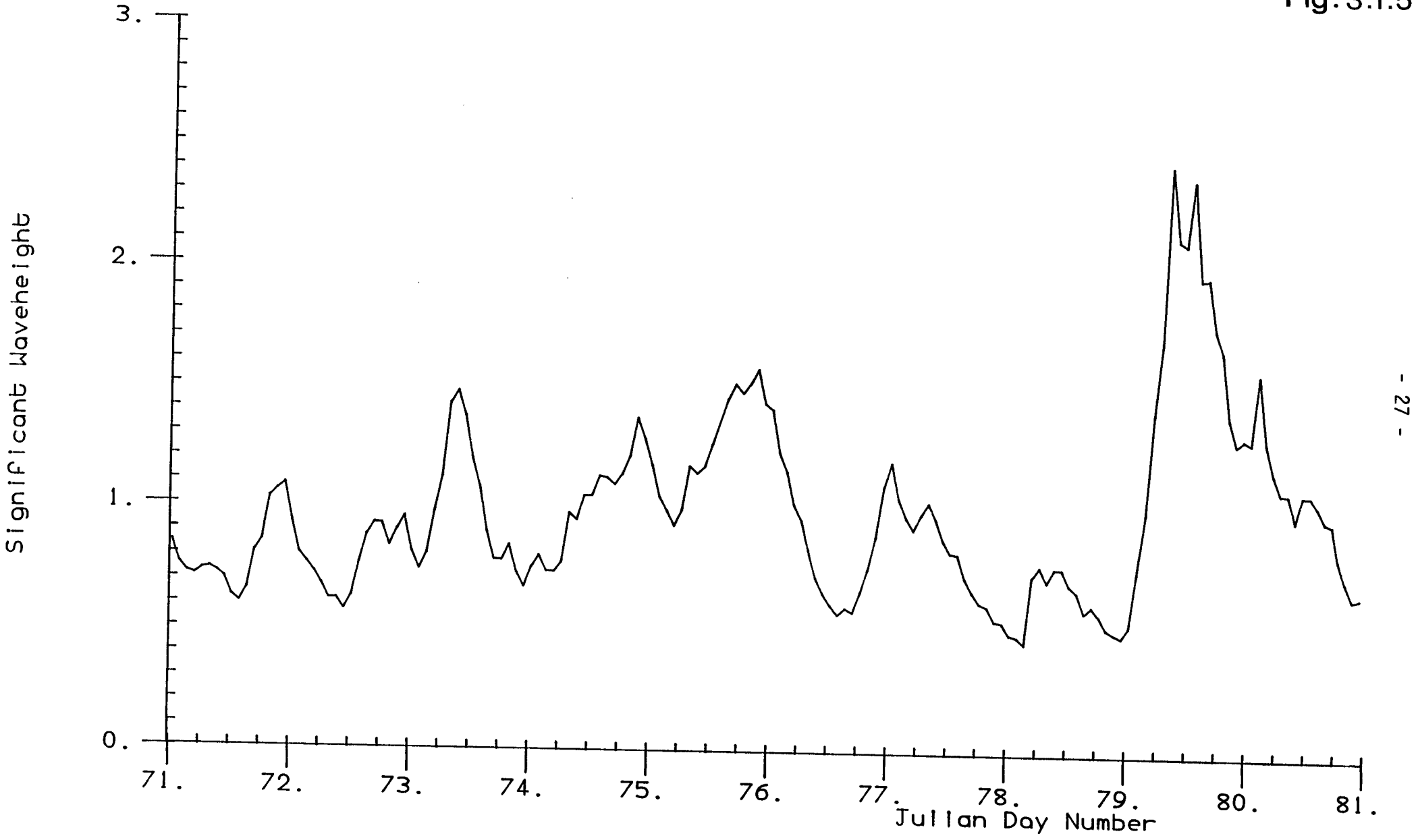

Flamborough Head - 1986

Fig. 3.1.6

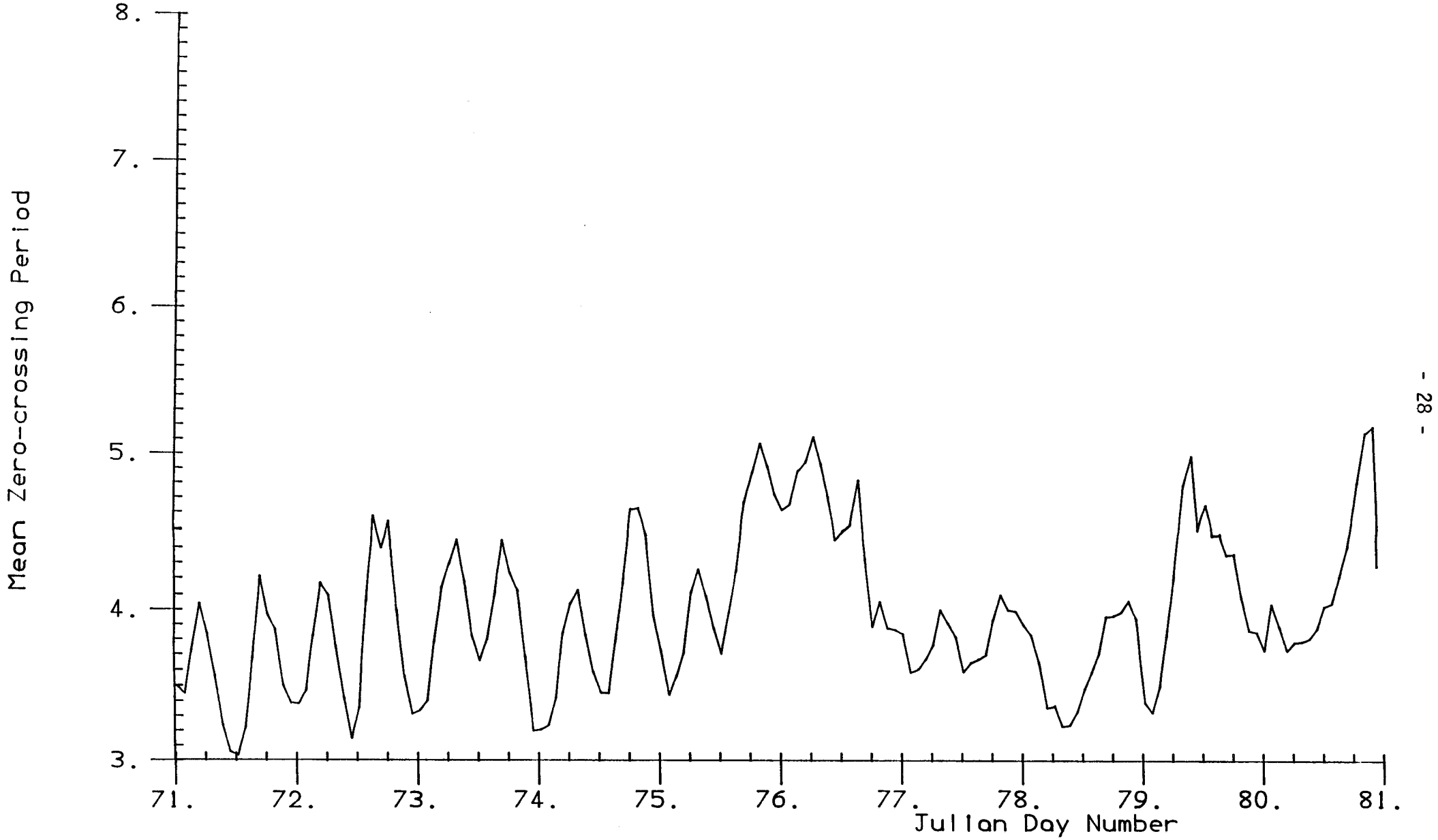

Flamborough Head -1986

Fig.3.1.7

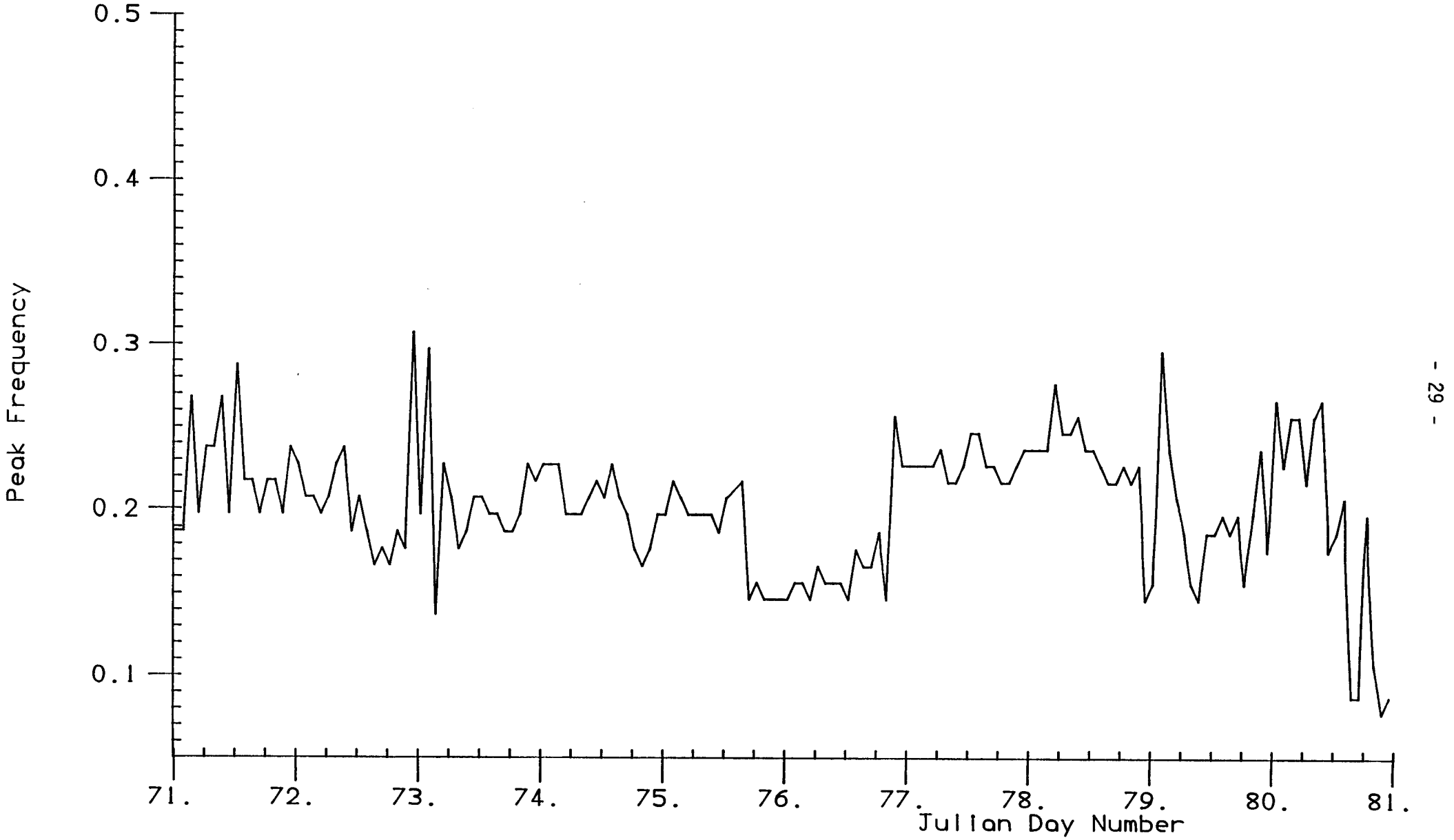

Flamborough Head - 1986

Fig. 3.1.8

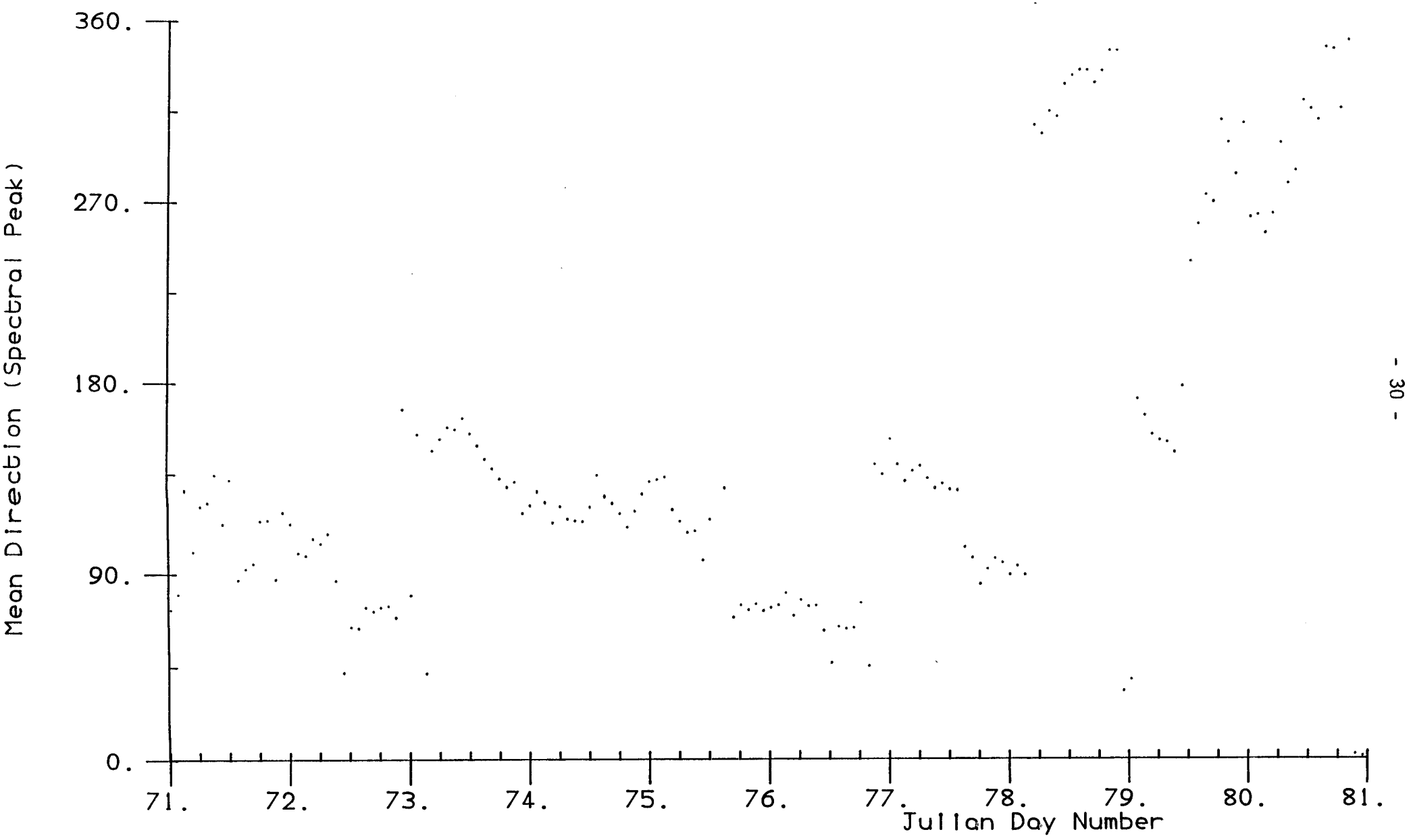

Flamborough Head -1986

Fig.3.1.9

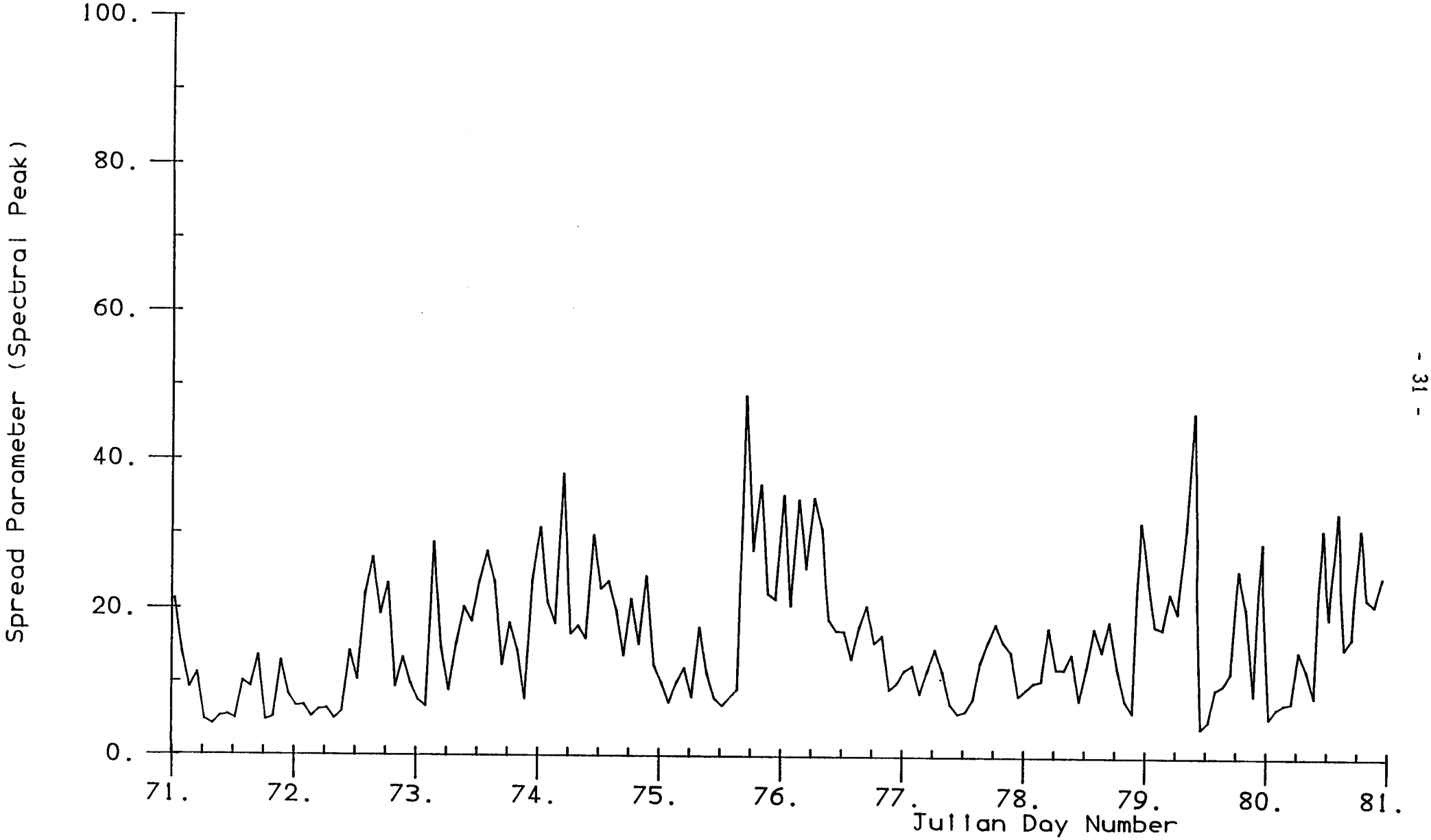

Flamborough Head -1986

Fig. 3.1.10

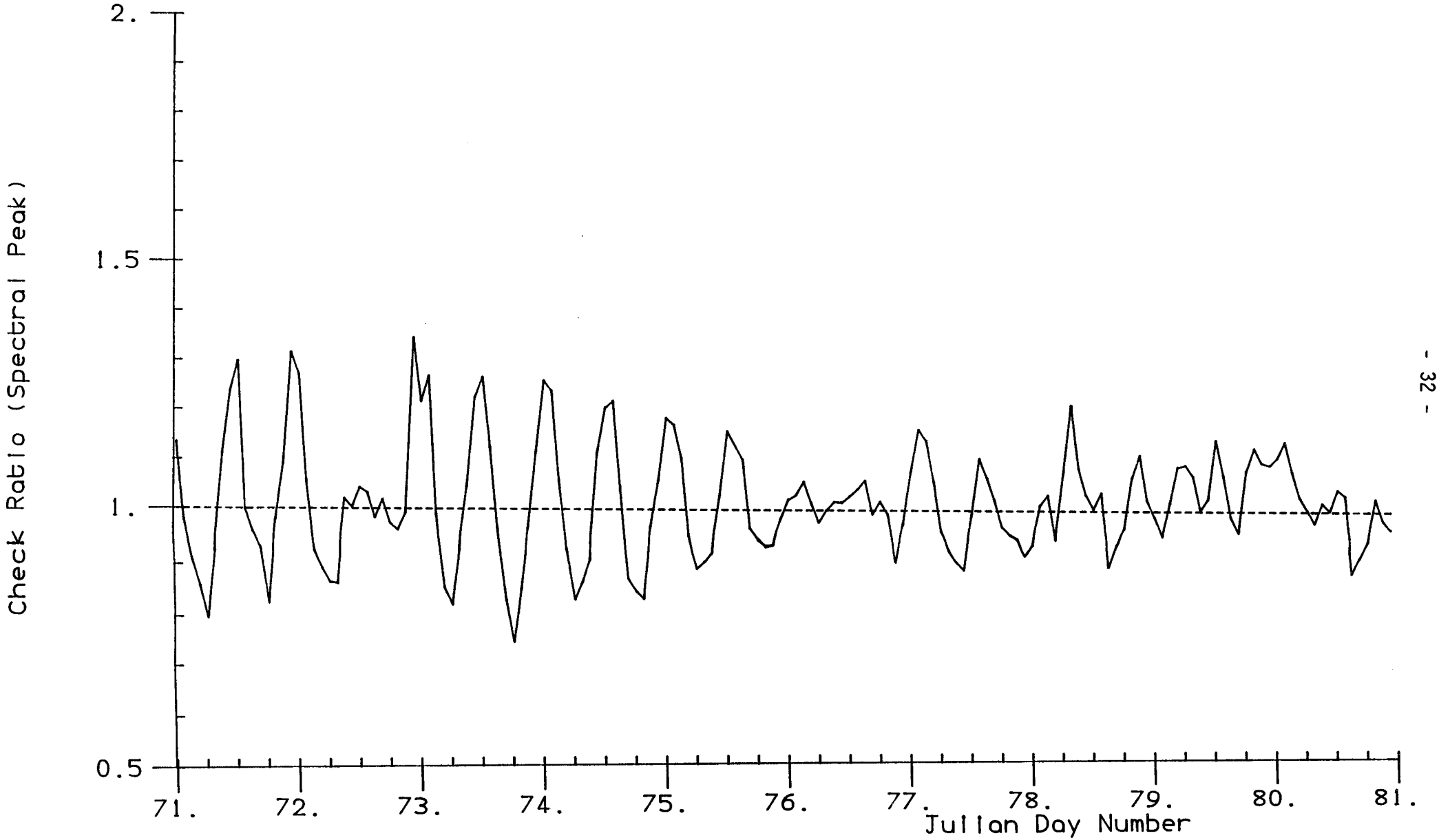

Flamborough Head - 1986

Fig. 3.1.11

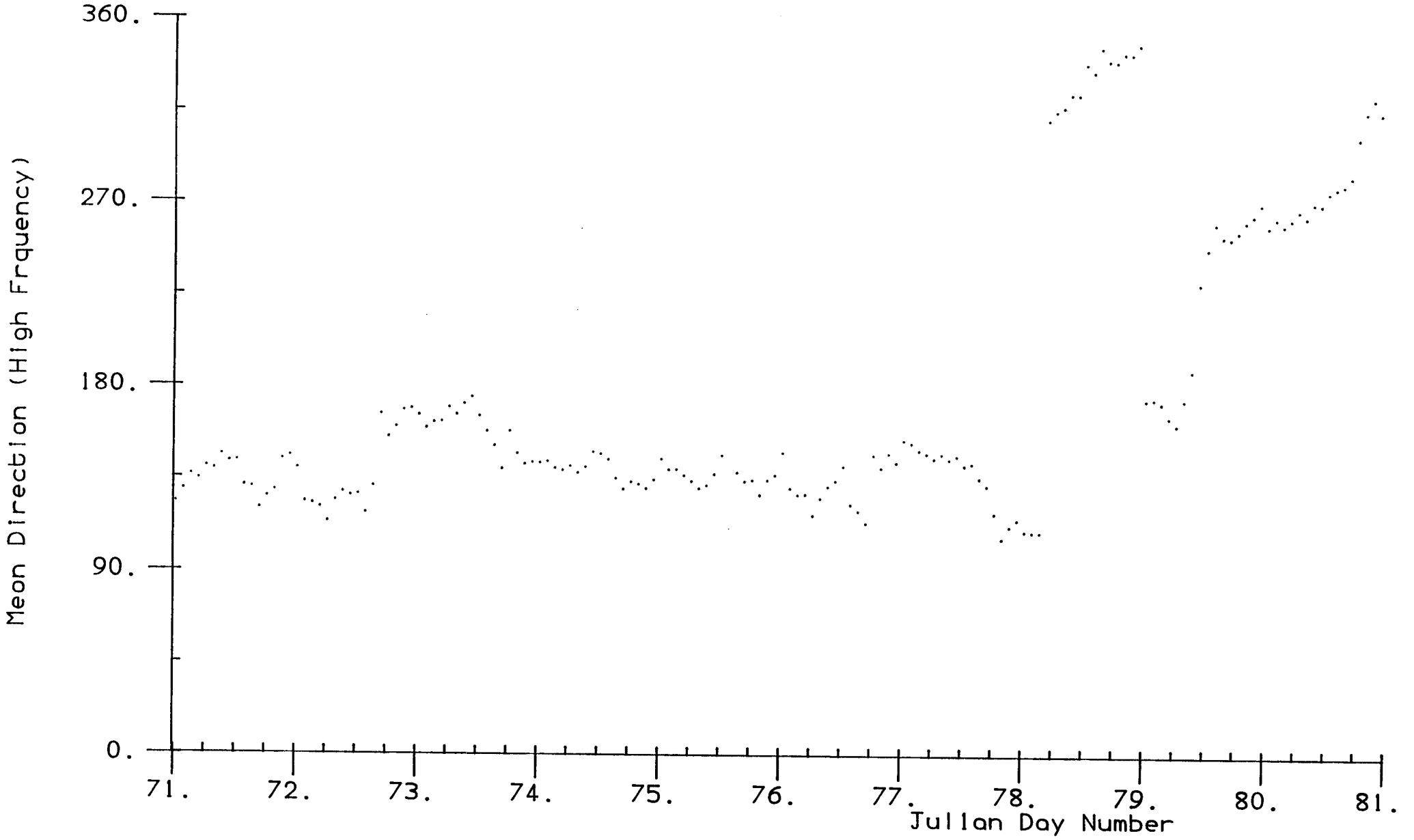

Flamborough Head - 1986

Fig. 3.1.12

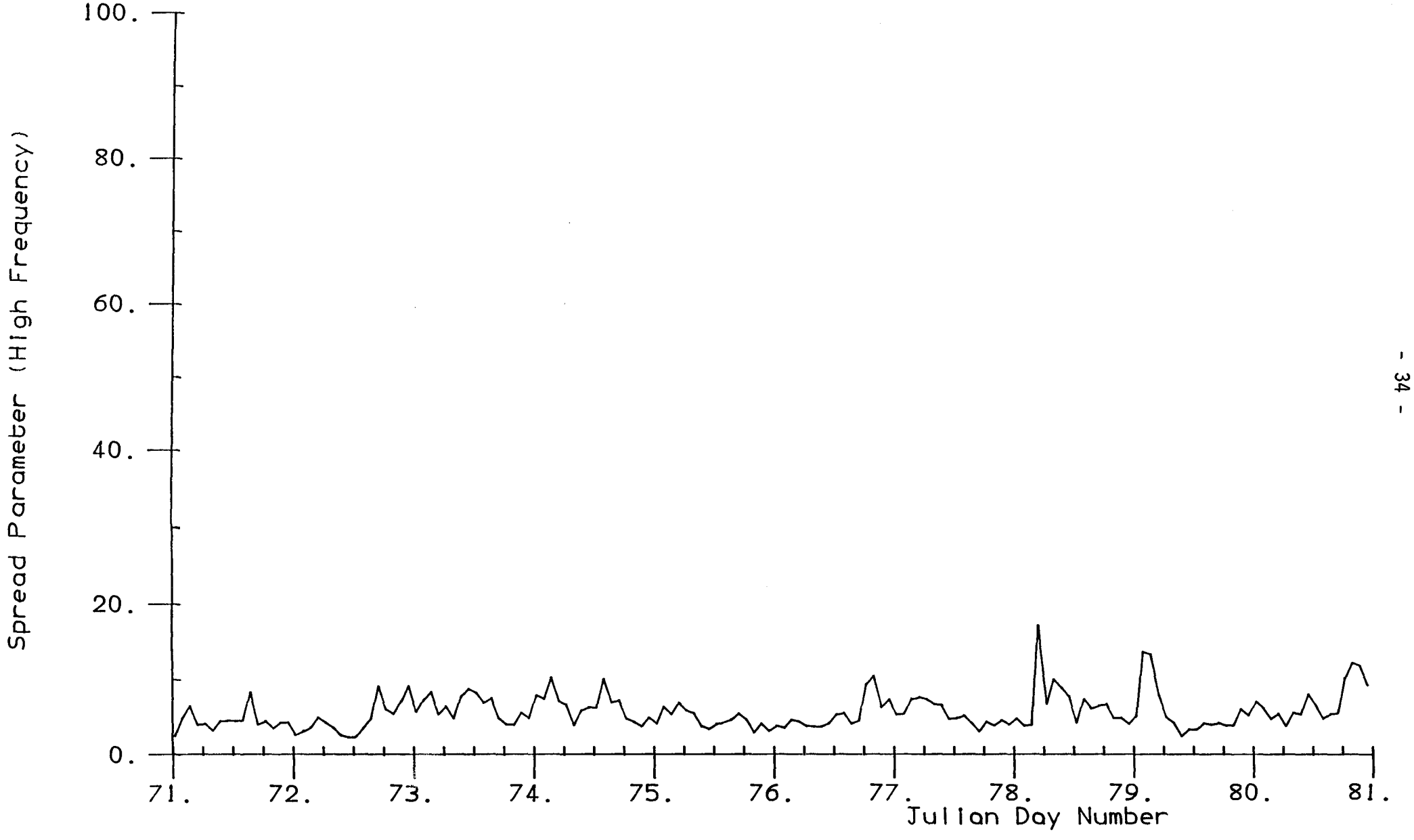

Flamborough Head - 1986

Fig. 3.1.13

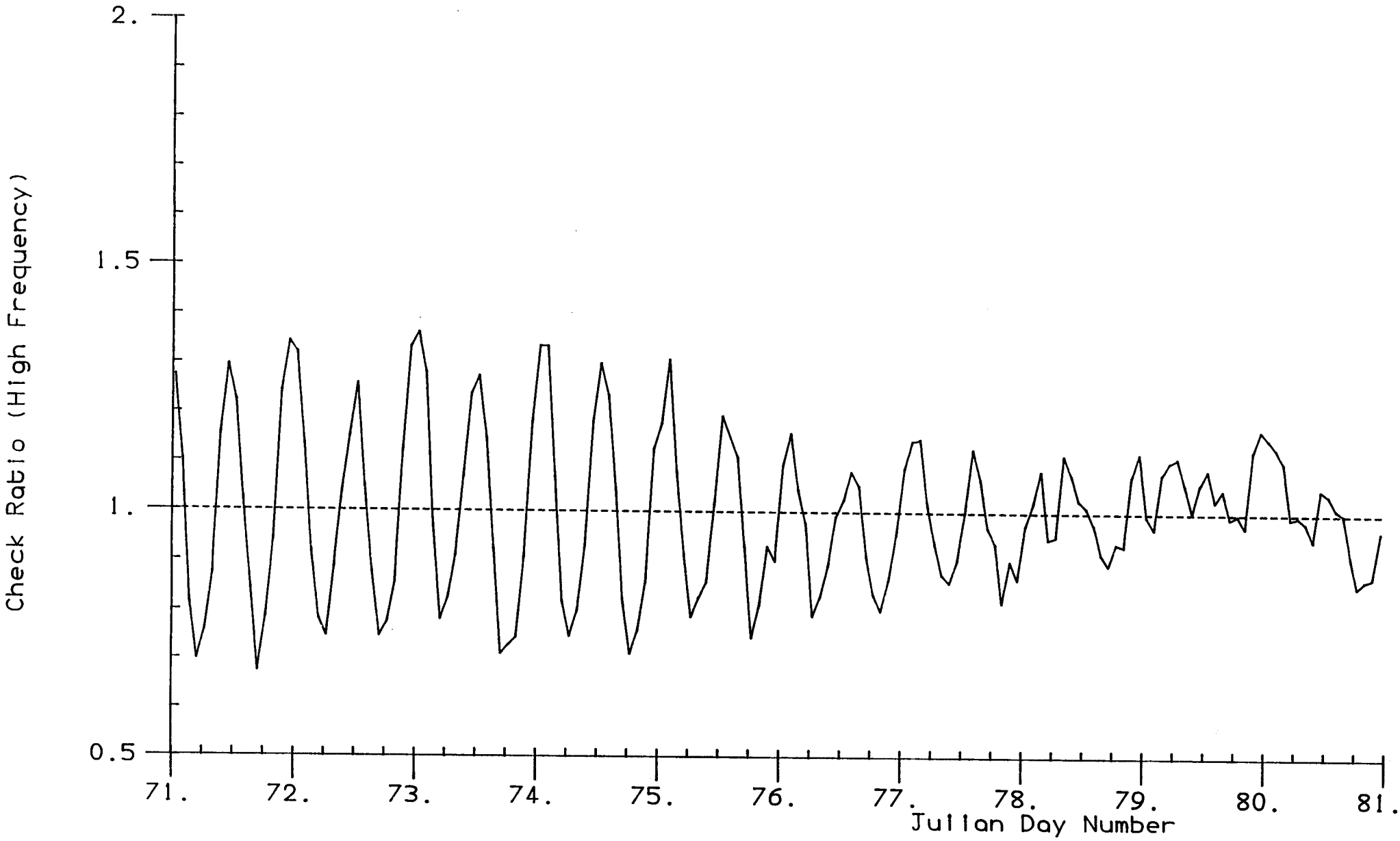

Flamborough Head - 1986

Fig. 3.1.14

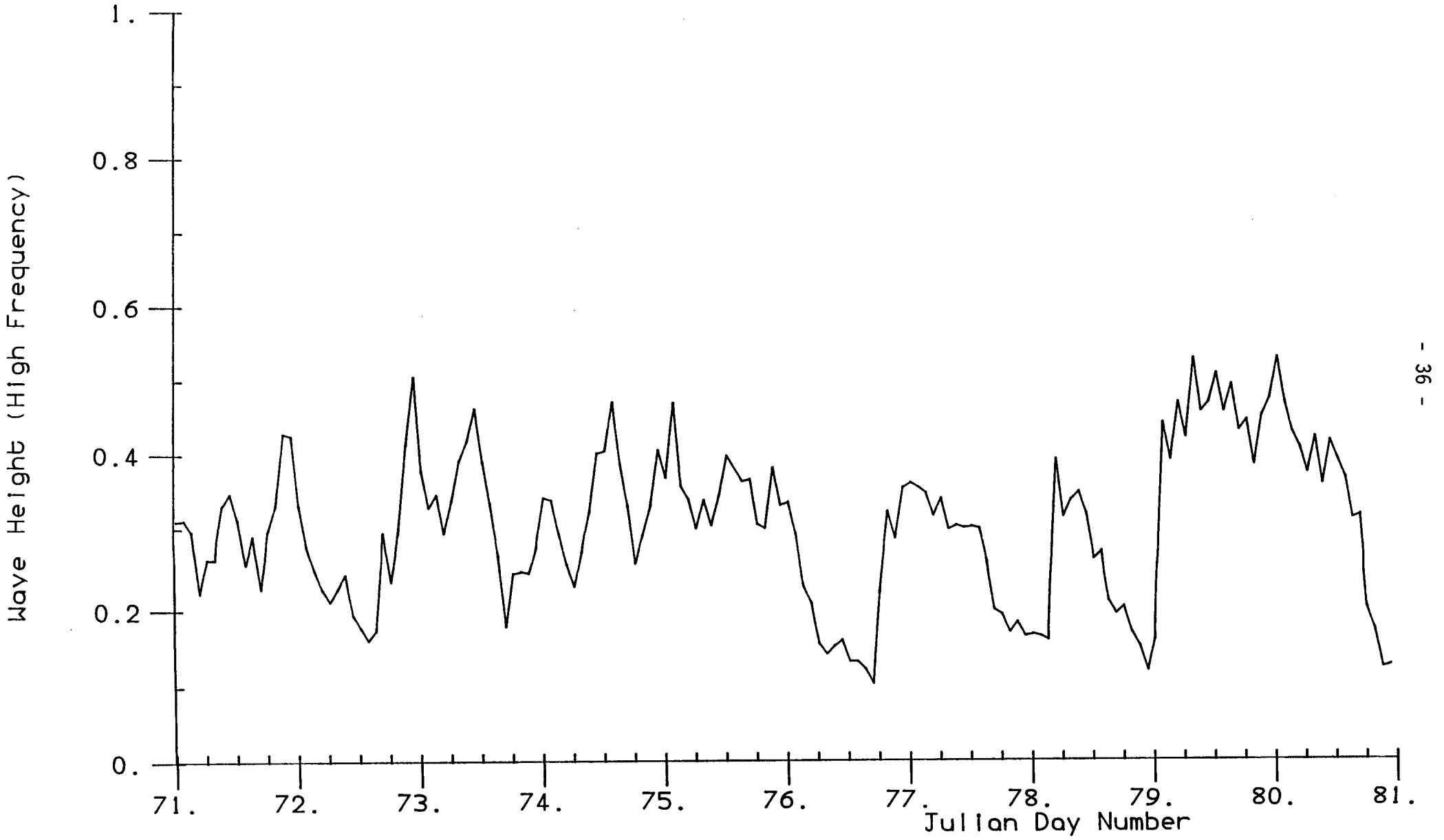

South-West Approaches 1986

Fig. 3.2.1

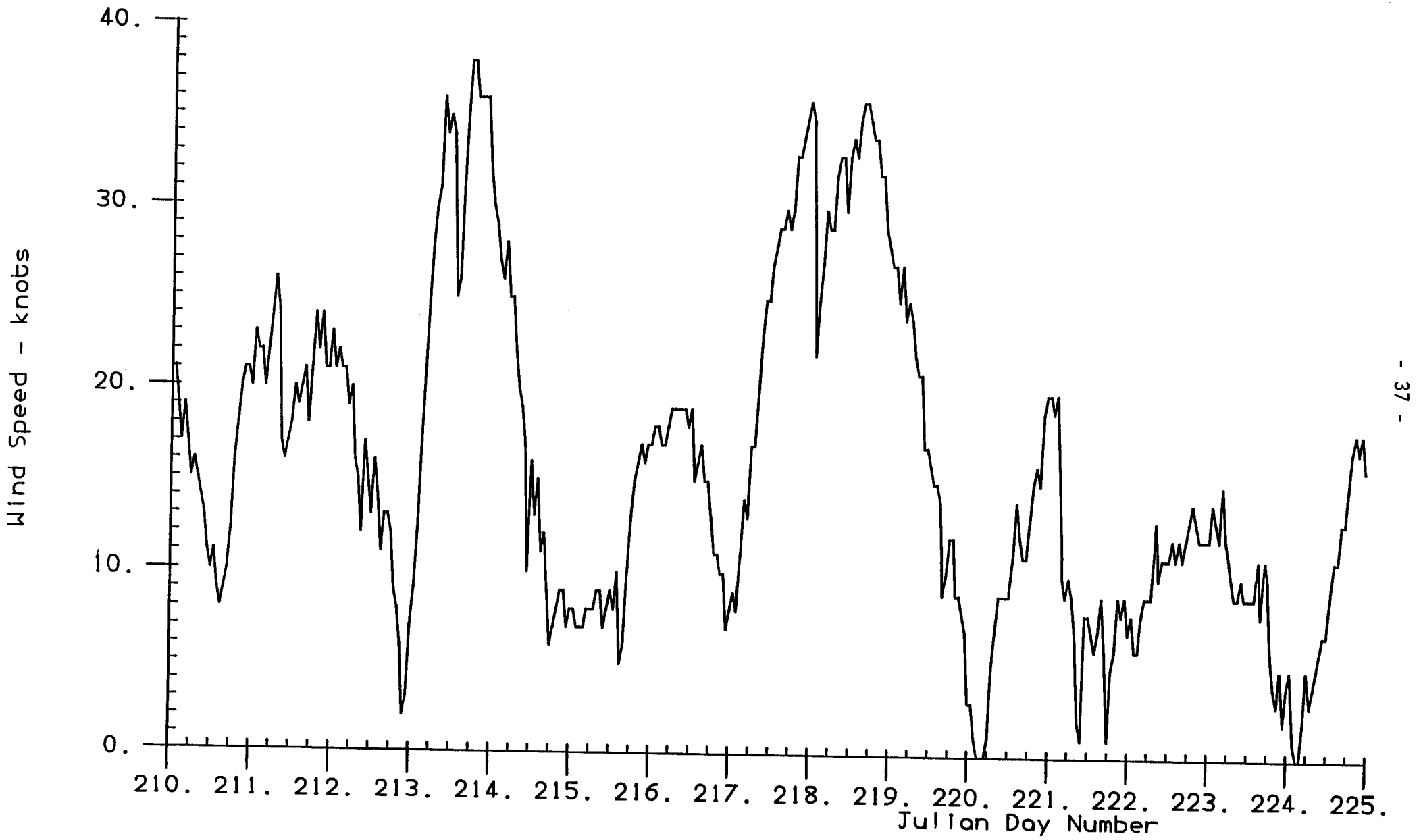

South-West Approaches 1986

Fig. 3.2.2

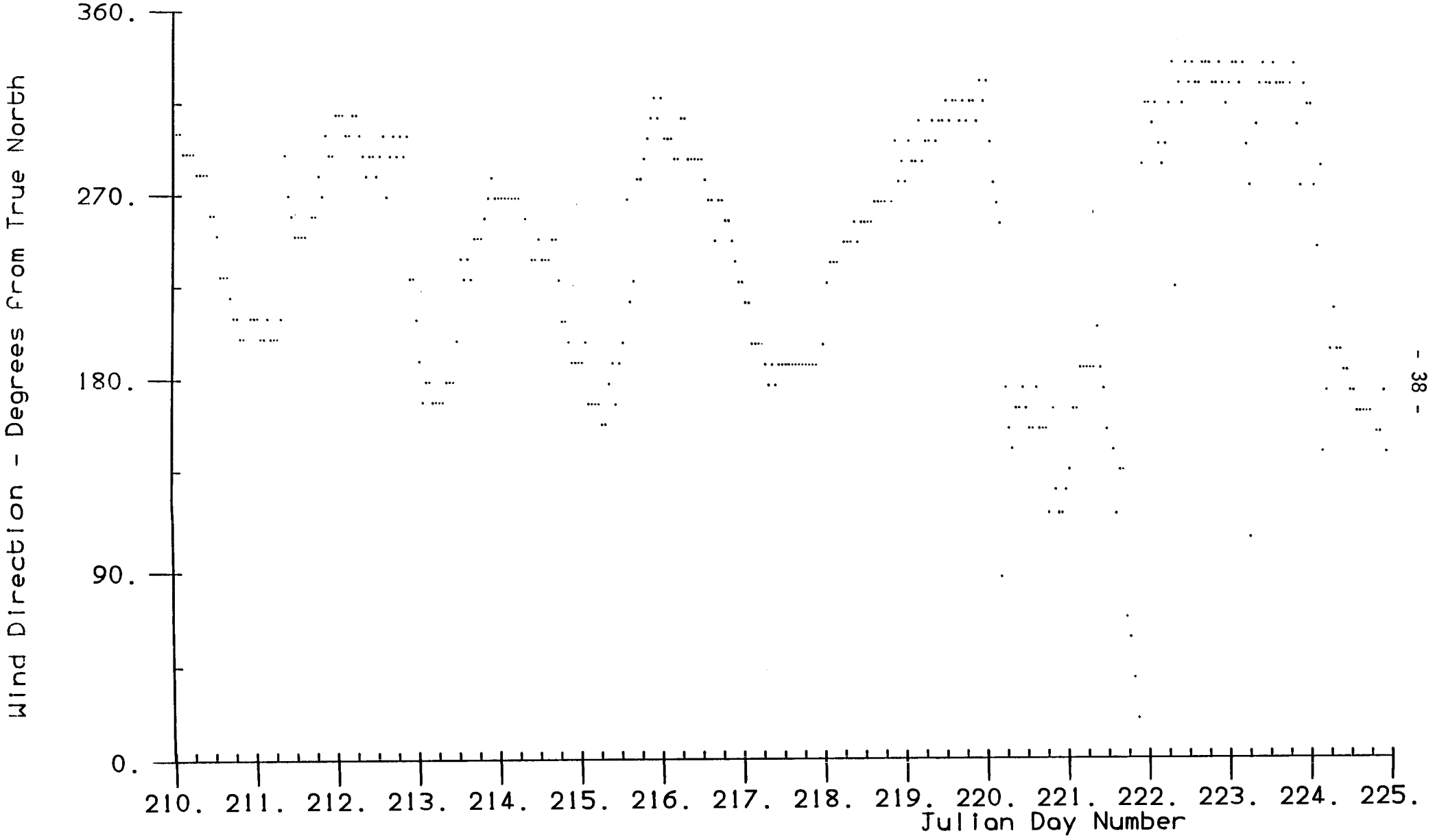

South-West Approaches 1986

Fig. 3.2.3

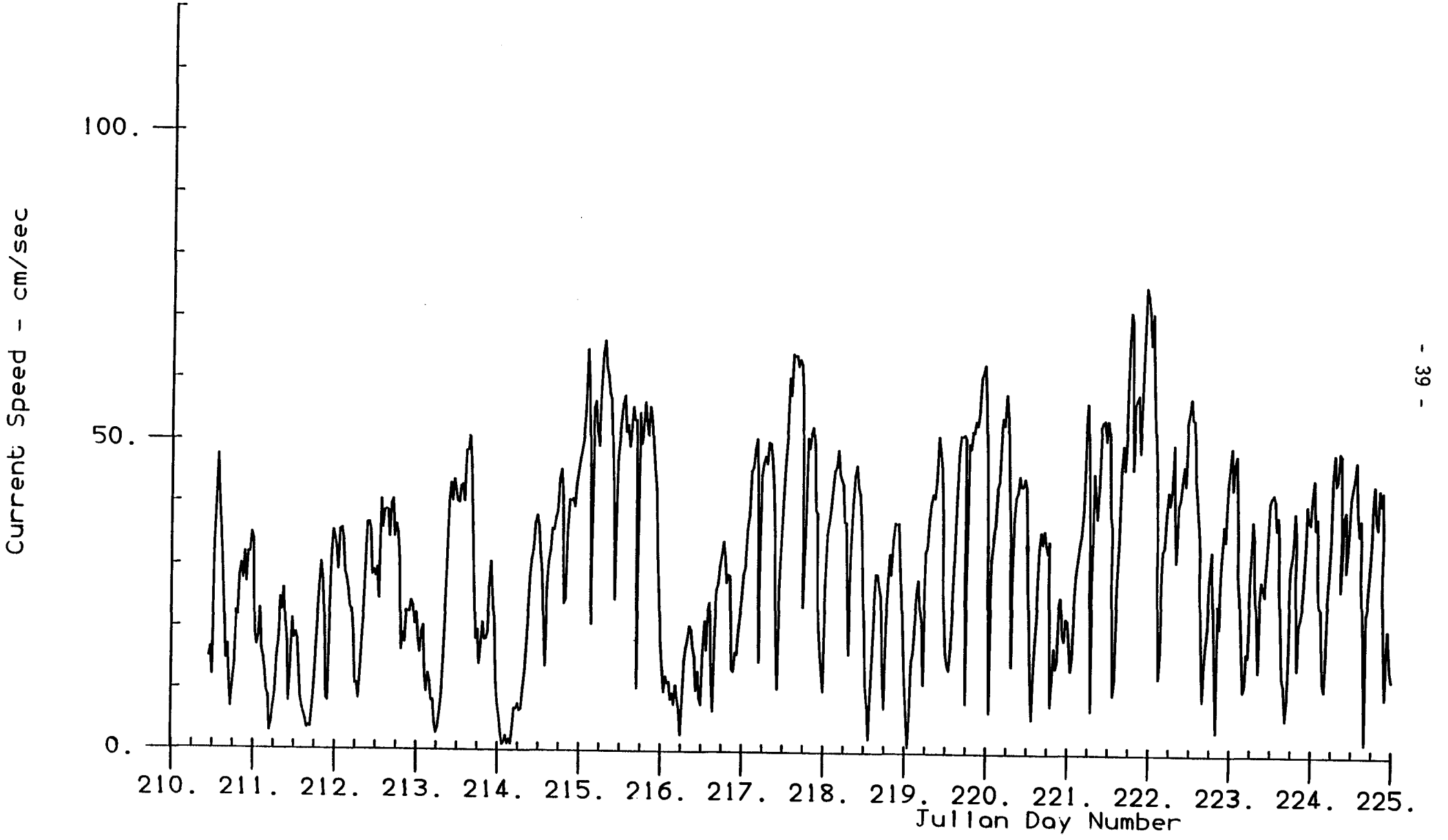

South-West Approaches 1986

Fig.3.2.4

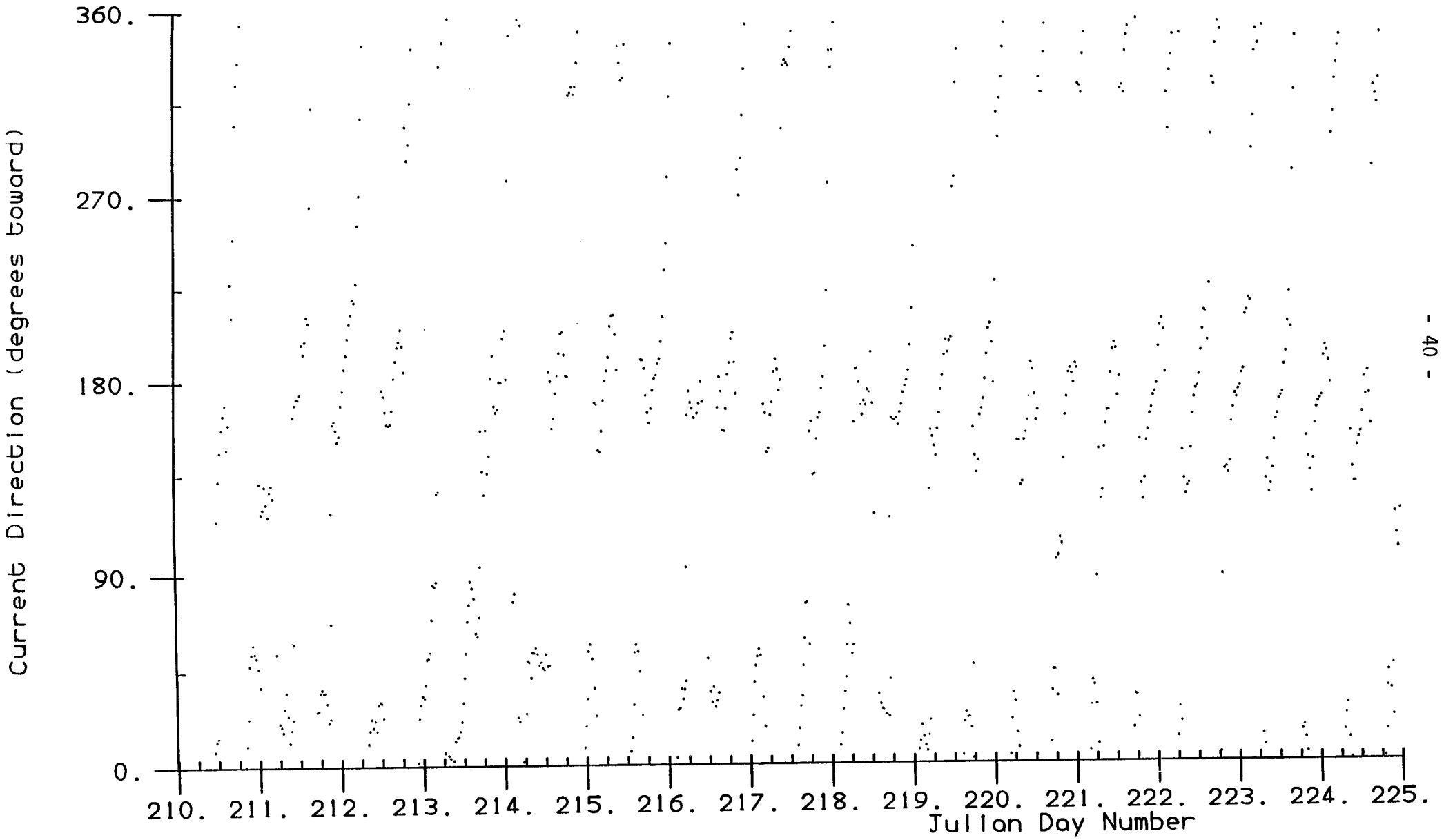

South-West Approaches 1986

Fig. 3.2.5

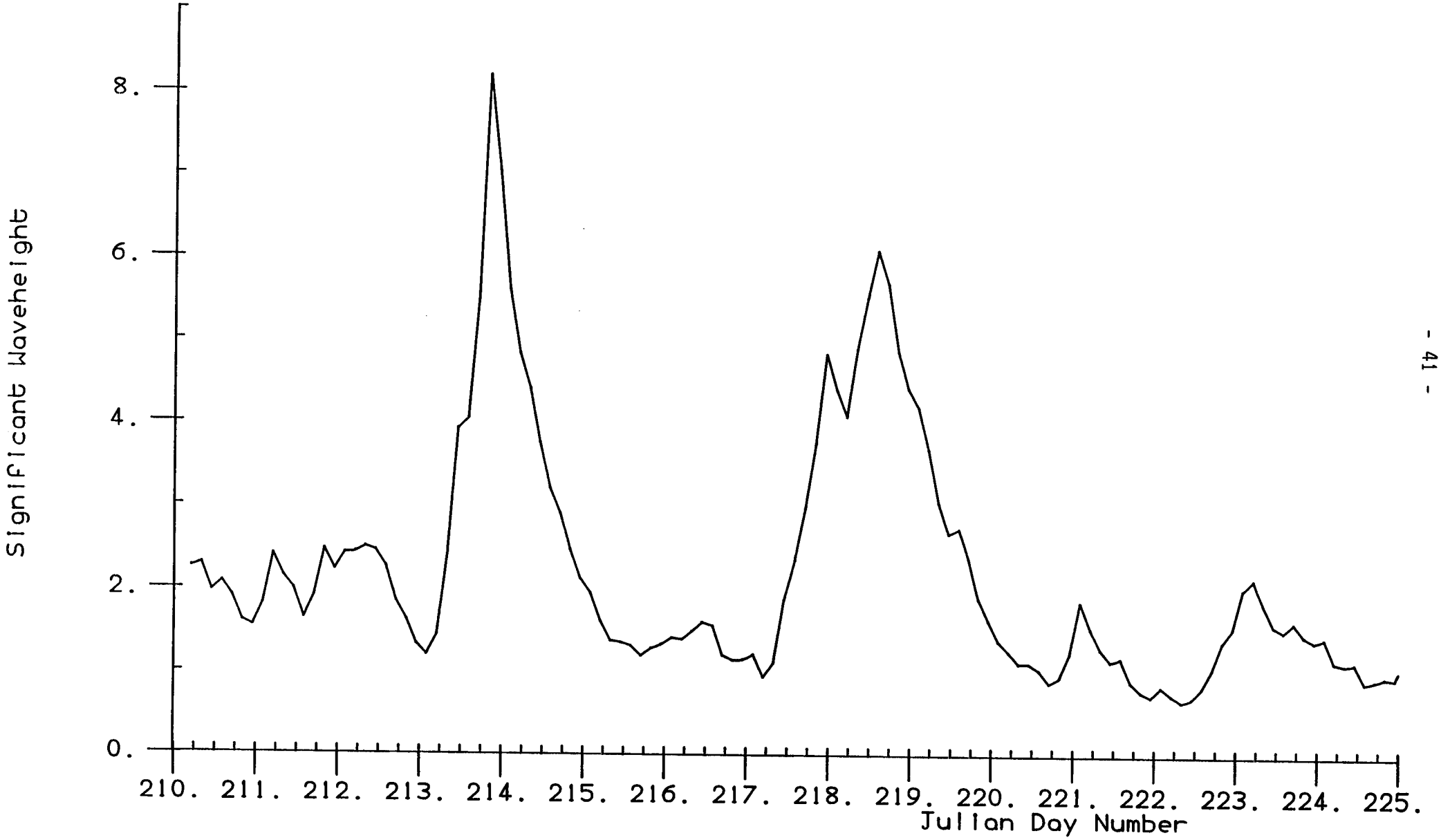

South-West Approaches 1986

Fig. 3.2.6

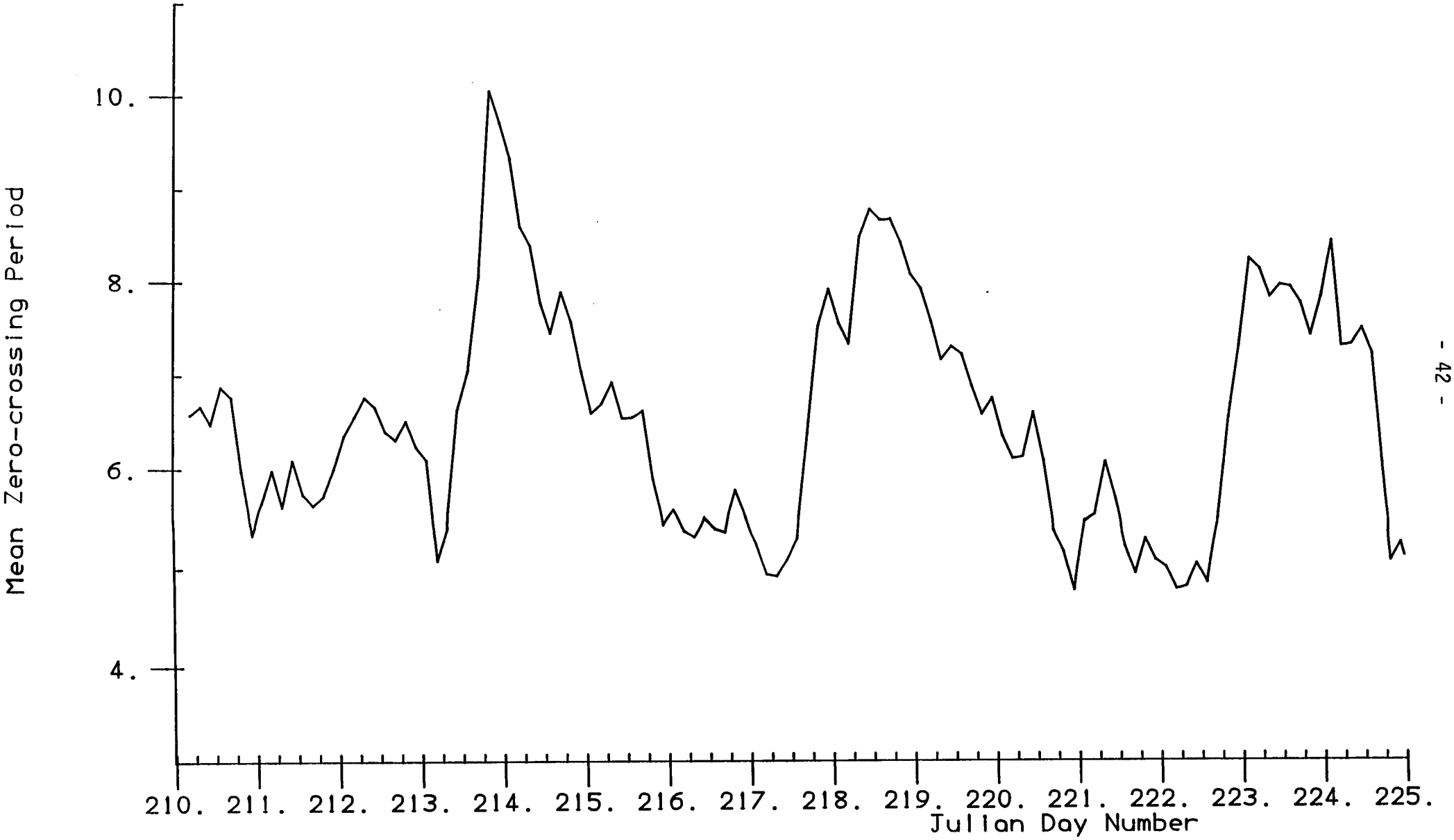

South-West Approaches 1986

Fig. 3.2.7

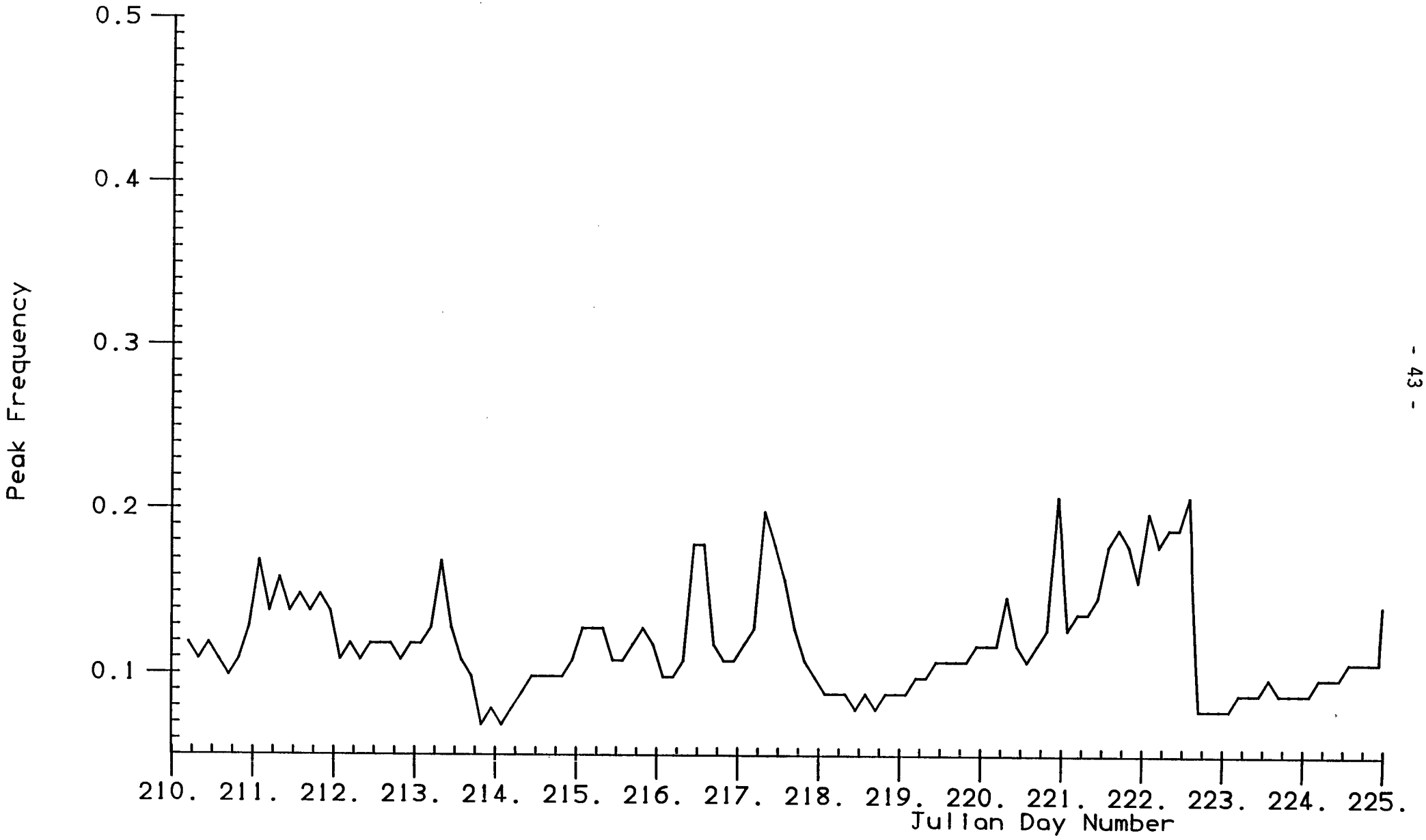

South-West Approaches 1986

Fig. 3.2.8

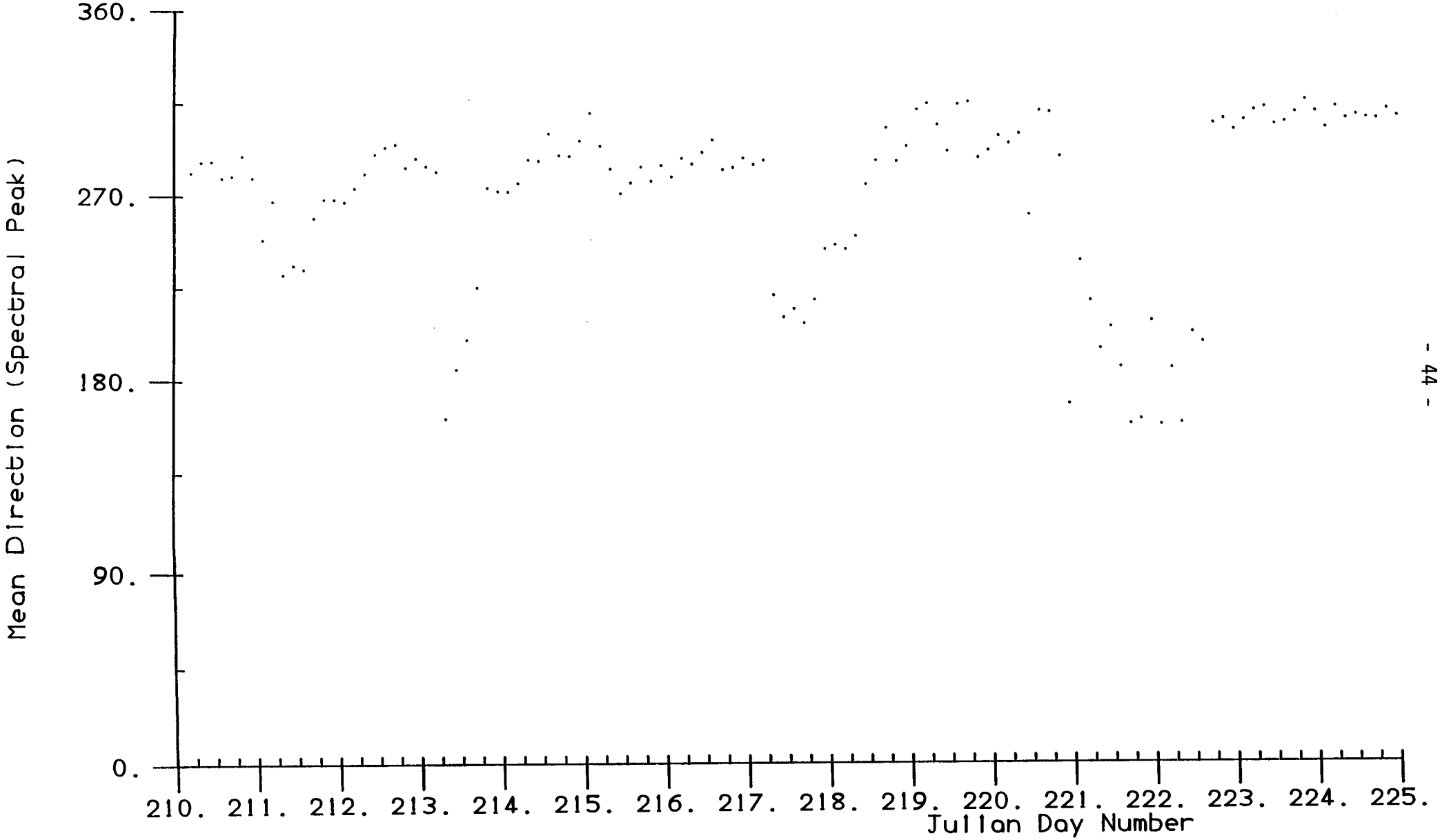

South-West Approaches 1986

Fig. 3.2.9

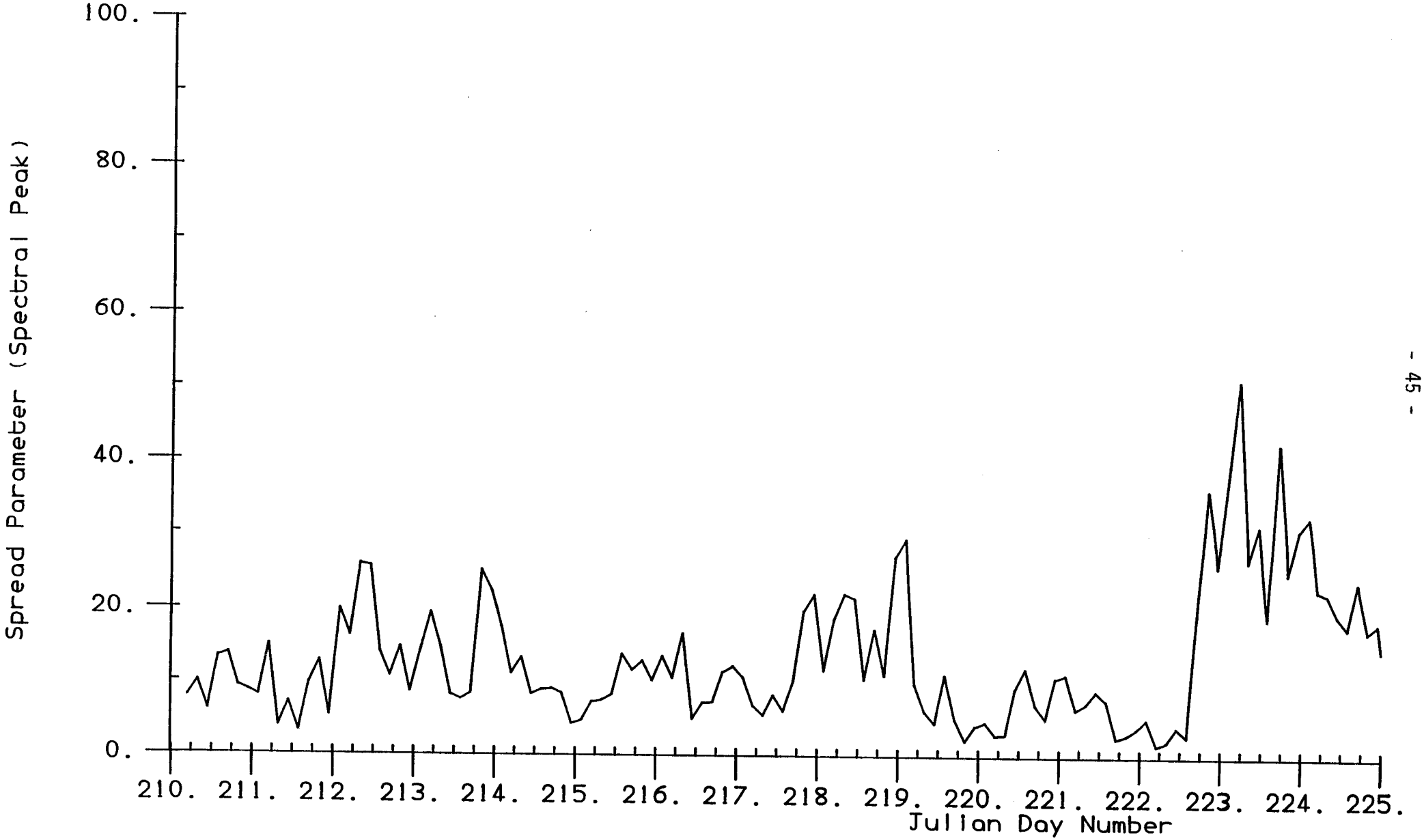

South-West Approaches 1986

Fig. 3.2.10

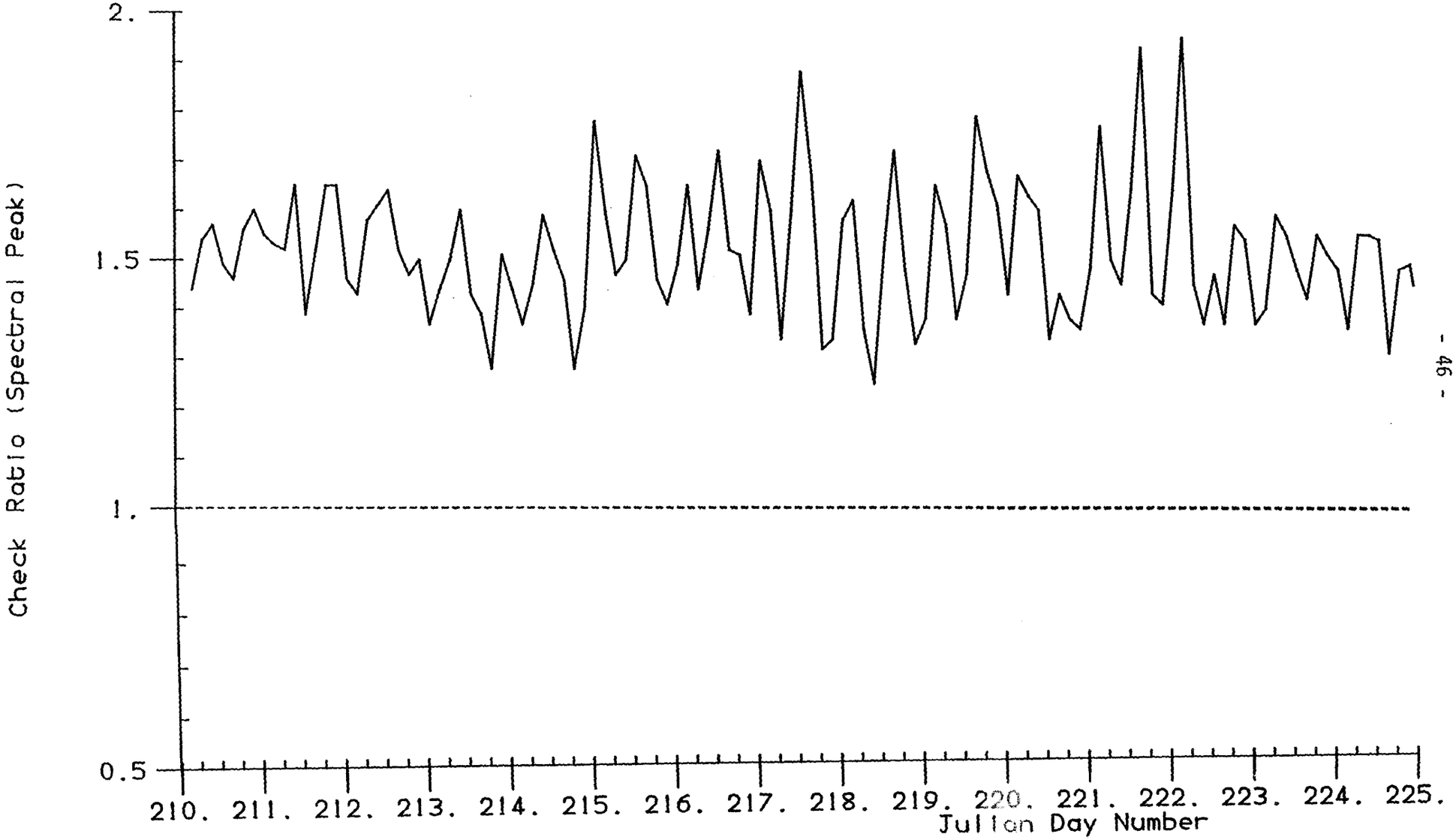

South-West Approaches 1986

Fig. 3.2.11

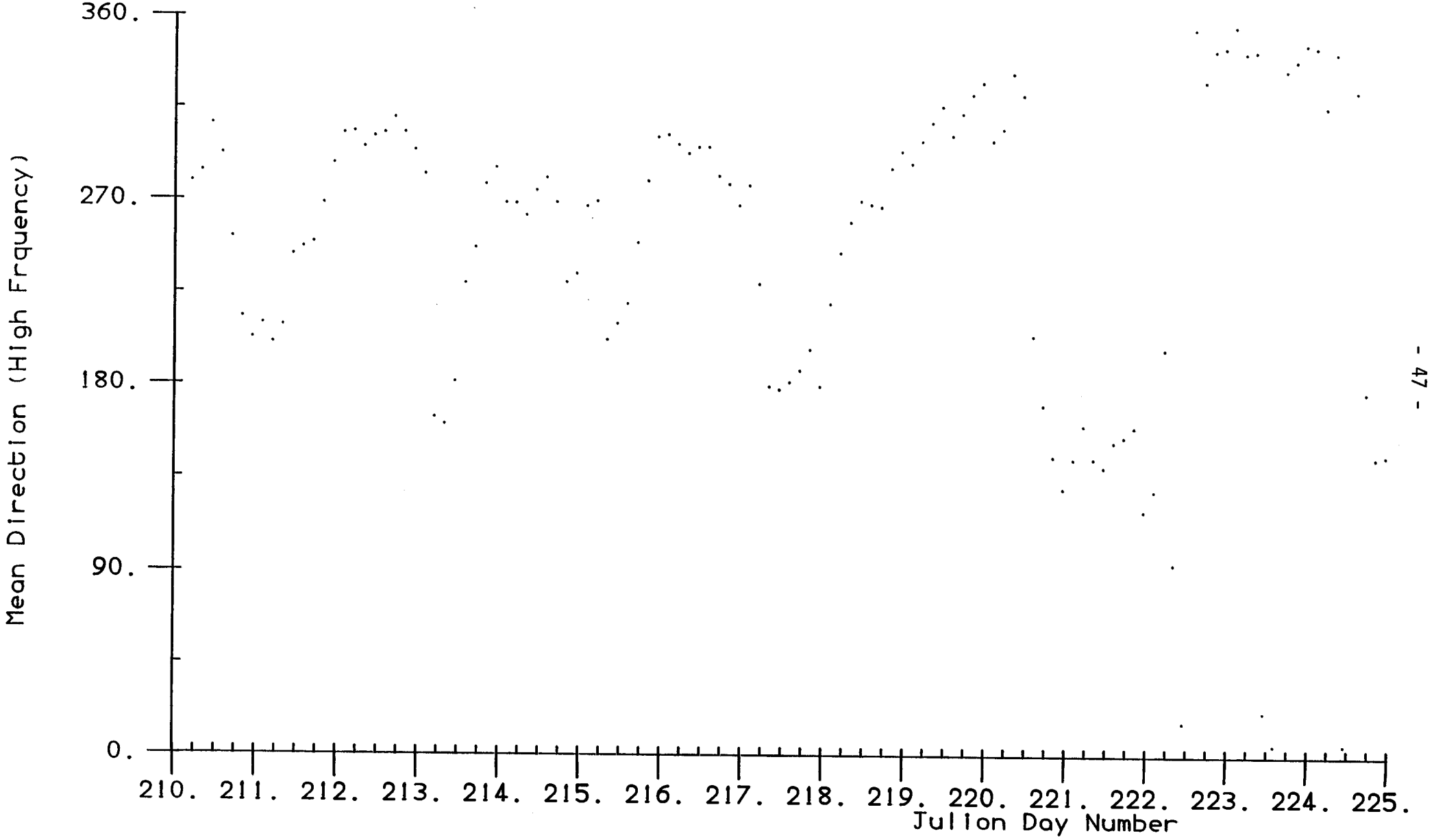

South-West Approaches 1986

Fig.3.2.12

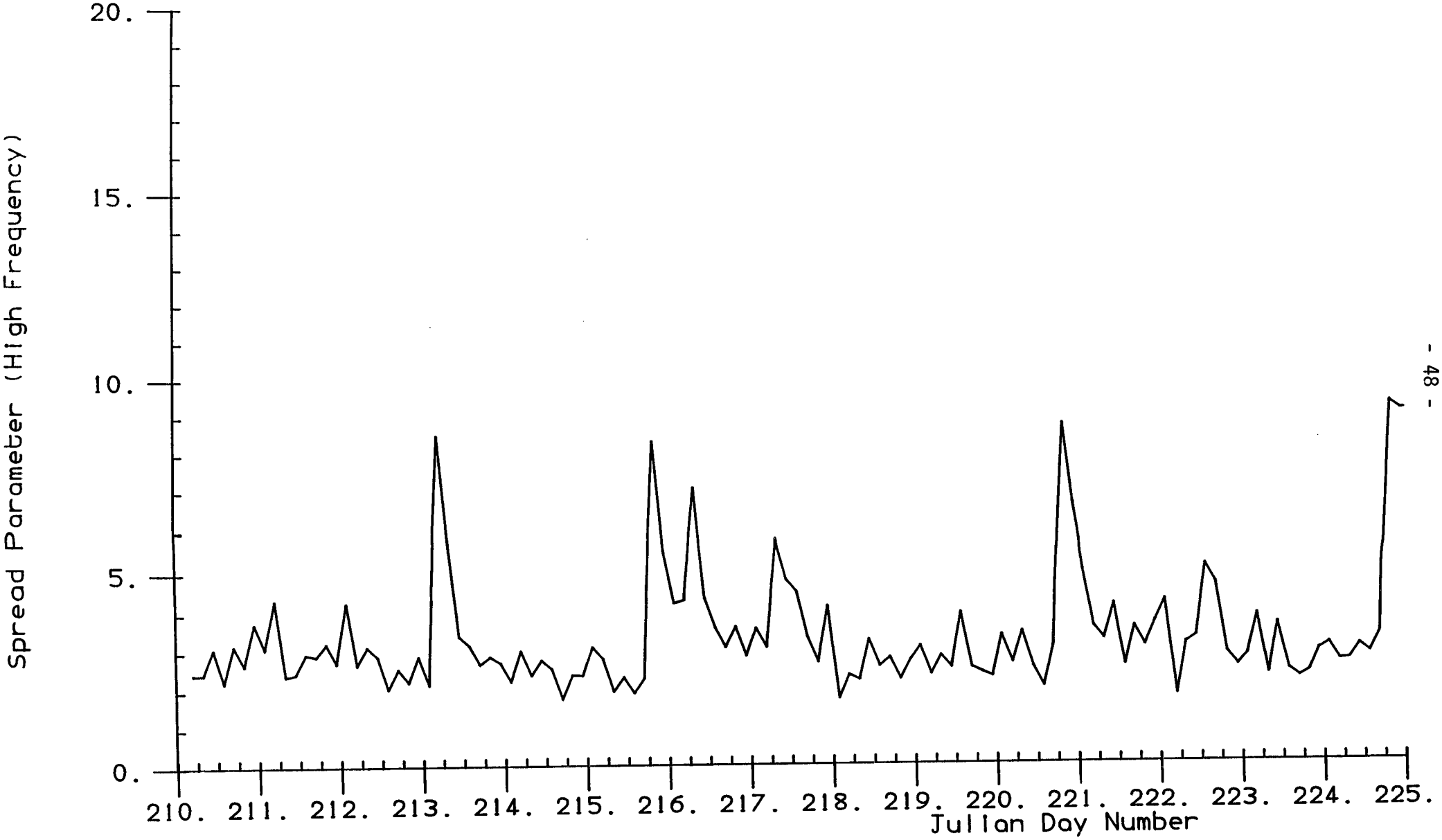

South-West Approaches 1986

Fig. 3.2.13

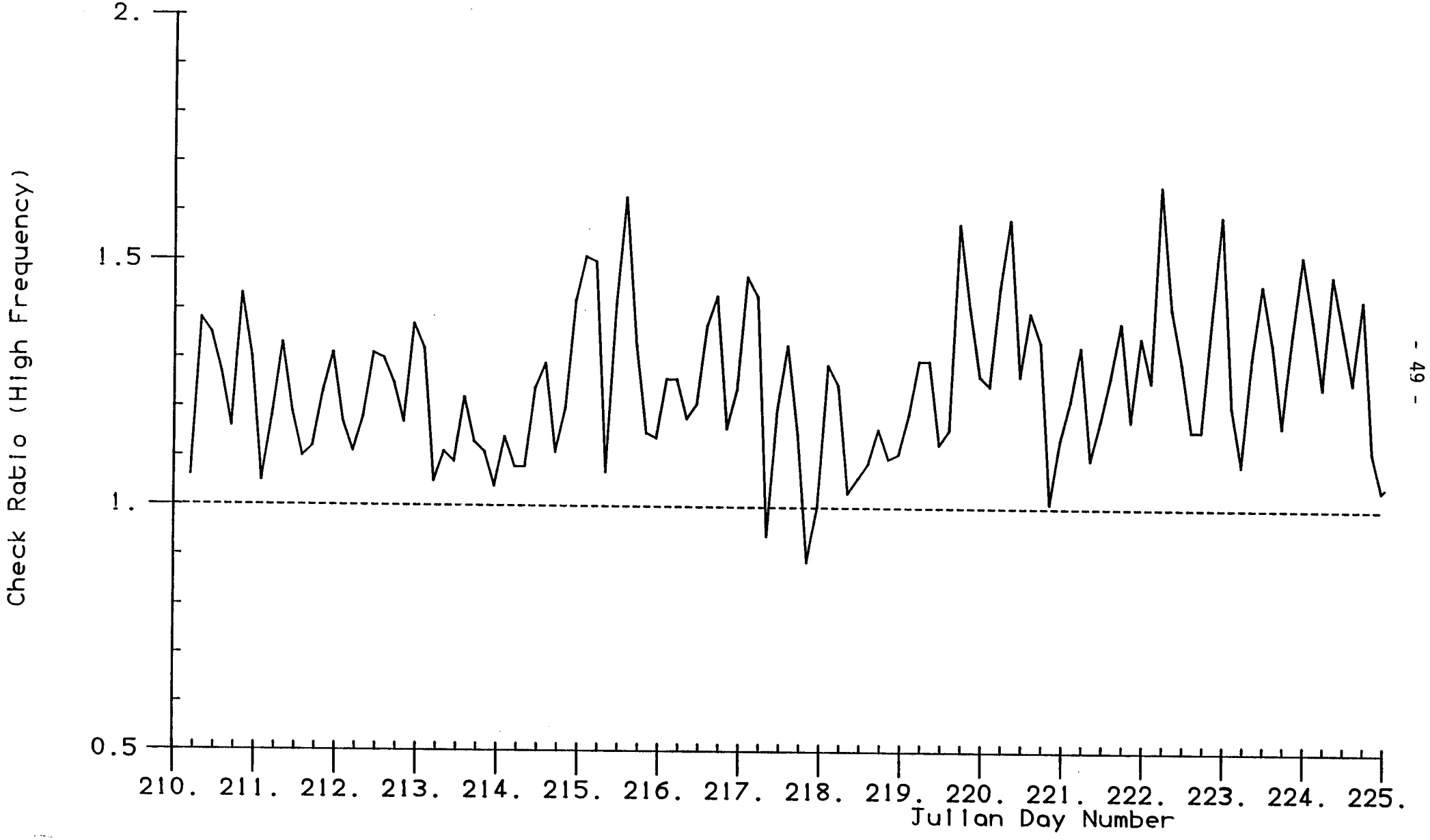

South-West Approaches 1986

Fig. 3.2.14

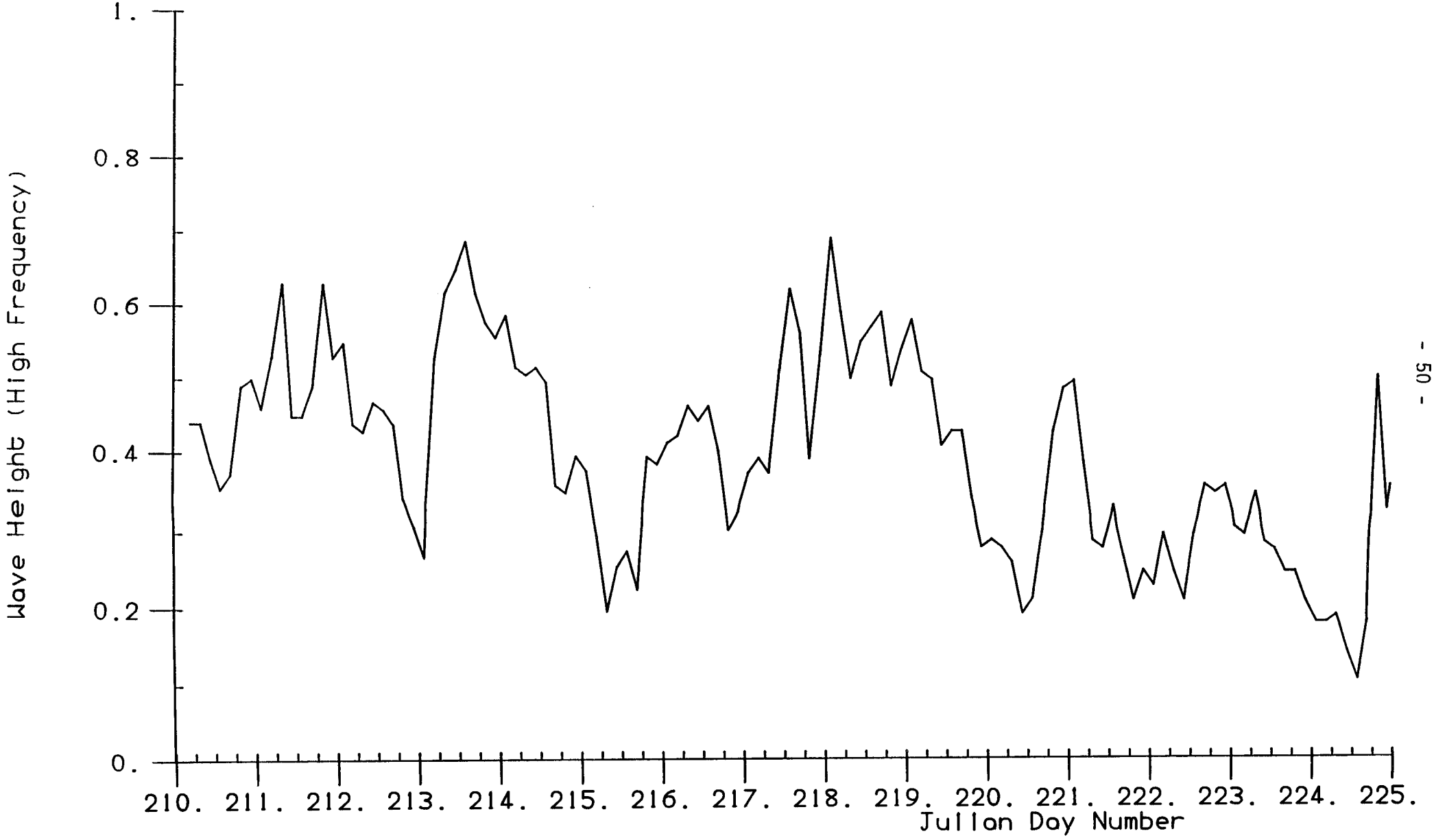

4. COMPARISON OF SURFACE CURRENTS MEASURED BY HF RADAR (OSCR) AND A MOORED SURFACE BUOY

4.1 Comparisons with H.F. Radar (OSCR)

The surface current buoy deployment (Table 4.1) spanned a period during which a series of measurements were made using the remote Ocean Surface Current Radar (OSCR) technique. The measurements were made on behalf of the Department of Energy by Marex Ltd, and had been designed to provide field data for the testing of a new algorithm for extracting wave information.

Instrument	Depth (m)	Record Start (Day No.)	Record End (Day No.)	Sampling Interval (s)	Parameters
VAESAT2	1.0	40.4	85.5	60	V_E, V_N, T

Table 4.1 Details of the surface current buoy deployed near 54°14'N, 0°0.5'W

Near surface currents were measured at 1 m depth beneath a surface following buoy (Collar et al., 1987) moored (fig. 4.1) at 54°14'N, 0°0.5'W, approximately 2 km due West of the Wavec buoy position. A diagram of the mooring is shown in fig. 4.2. The data obtained, details of which are given in Table 4.1, were of good quality and spanned 45 days. Unfortunately the installation of the mooring coincided with the disappearance of the Wavec buoy following trawling activities in the area. This was located and retrieved but it was not reinstated until Day 70. Hence the joint current-wave analyses covered only the period between Days 71-80, the surface current buoy itself being trawled on Day 85. It was felt that the current data available from the deployment offered a valuable opportunity to make a preliminary assessment of the potential of the radar for obtaining observations relevant to future coastal erosion programmes: arrangements were accordingly made for IOS to have access to the current data set. The principle of surface current radar is

discussed in Shearman (1981). In brief, each OSCR station transmits a wide angle beam at approximately 27 MHz and receives backscattered signals on a number of 1.2° beams each separated by 6°. The signal returned along each beam is due to resonant (Bragg) backscatter from sea waves of half the radar wavelength, and is Doppler-shifted due to motion of the waves. The signal is gated into range cells and a spectral analysis undertaken for each cell. The resulting spectrum consists of two dominant peaks at positive and negative Doppler frequencies corresponding to advancing and receding Bragg resonant waves. The radial current component is derived by assuming that any displacement of the two peaks from symmetrical positions above and below the nominal carrier frequency results solely from a linearly superimposed surface current.

In order to define the surface current vector, two OSCR shore stations are used. In the present experiment these were situated on Flamborough Head and at Gristhorpe (fig. 4.1). The beams which most nearly illuminated the surface buoy site were in the directions 088° (Gristhorpe) and 025° (Flamborough Head). The experiment was not specifically designed for this comparison, and the nearest beam intersection at which both OSCR time series were sufficiently long to make a worthwhile comparison was approximately 2 km from the buoy (fig. 4.2). Time series of current components from these OSCR beams are shown in fig. 4.3 a, b, c, d together with the equivalent current components measured by the buoy.

4.2 Discussion

The data series are clearly well correlated. In order to compare the series directly it was necessary to establish a common timebase. This was done by linear interpolation, and the OSCR-buoy differences are shown in fig. 4.4 a, b.

The differences were sometimes small - on Day 78 for example they were generally a few cm/s for both beams - but at other times were substantial. Both beams show a negative mean level, indicating that OSCR generally indicated weaker currents than did the buoy. During Days 72 and 73, and in particular from midday on Day 75 until around midnight on Day 76 there is a strong tidally related difference between the two techniques. The possibility

that such differences could be caused by spatial variability in the currents has been investigated by examining, for each beam, the radial currents in the adjacent two bins on each side of the intersection point. While there are differences between these bins, the overall pattern remains the same. We think it unlikely, therefore, that spatial variability is the primary cause of the differences recorded. It seems unlikely also that different responses of the two systems to wind related currents were a major source of differences observed. During the comparison period winds were generally light or moderate - reaching peaks of about 8 m/s on Days 73, 75 and 77 - and were from the SE quadrant. On Day 78 the wind became northerly for a few hours, reaching 7 m/s, before decreasing to zero then rising to a peak of 18 m/s from a westerly direction. With the exception of this last storm, when the data series can be expected to differ in view of the different system responses to vertical shear in the water column, the differences do not appear to be related primarily to wind, for throughout the comparison period the OSCR records a mean NE component relative to the buoy measurement.

Tidally related differences measured at Gristhorpe and Flamborough were of the same phase and of similar magnitude. When allowance is made for the fact that the currents measured in each of the two principal tidal directions by the OSCR stations appear in antiphase, it becomes clear that for both OSCR stations the OSCR underreads compared with the buoy when the resolved current component is towards the beam (positive) and overreads in a comparative sense when the resolved component is directed away from the station. The reasons for this are at present unclear. The tidally related differences are particularly noticeable on days 75 and 76 (fig. 4.4a) and these coincide with a period of about 30 hours when wind and significant wave height dropped suddenly and wave activity was dominated by a low swell propagating down the North Sea (see fig. 3.1.7).

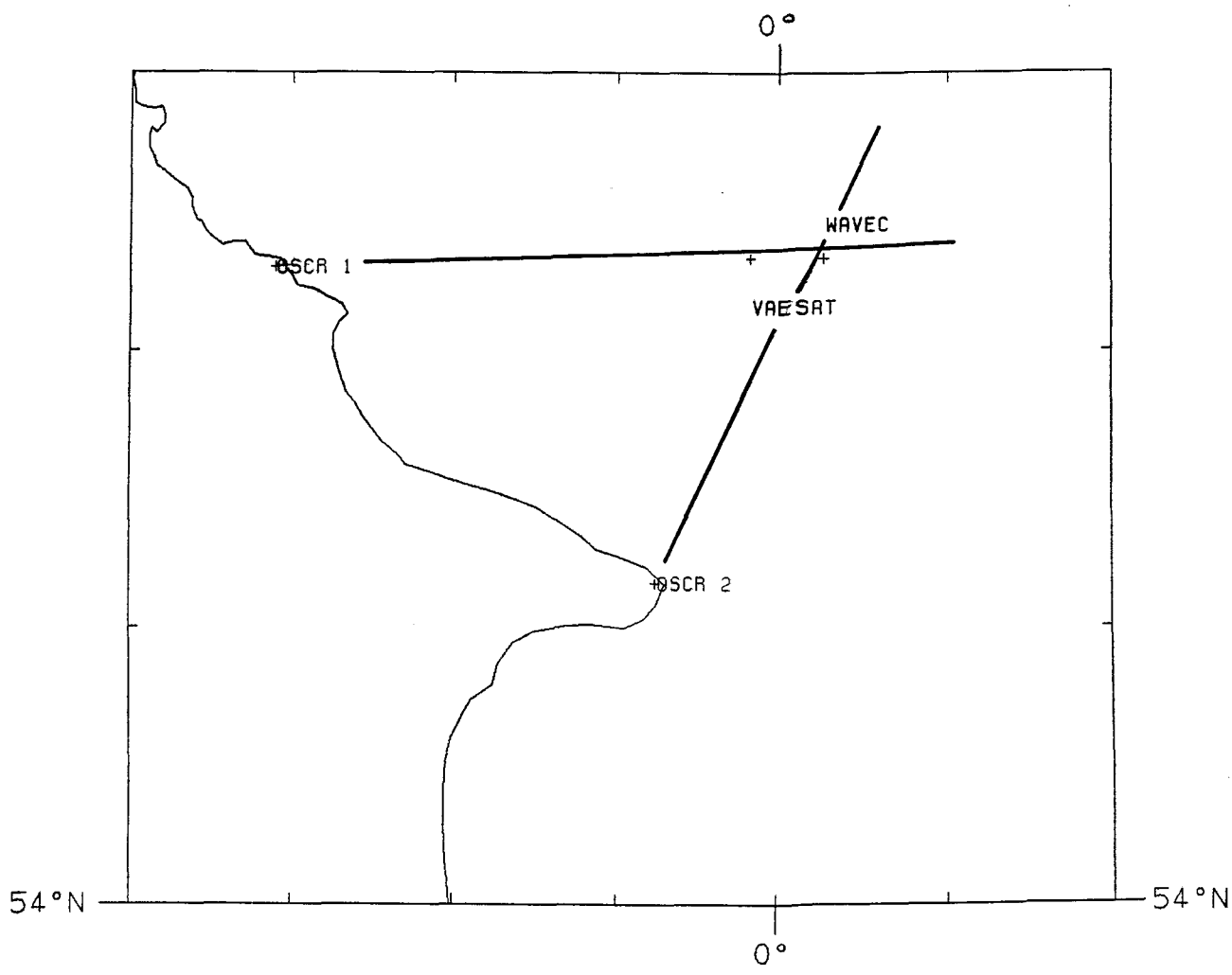

Figure 4.1 Flamborough mooring site showing current and wave measuring buoy positions and directions of OSCR beams used in the comparison.

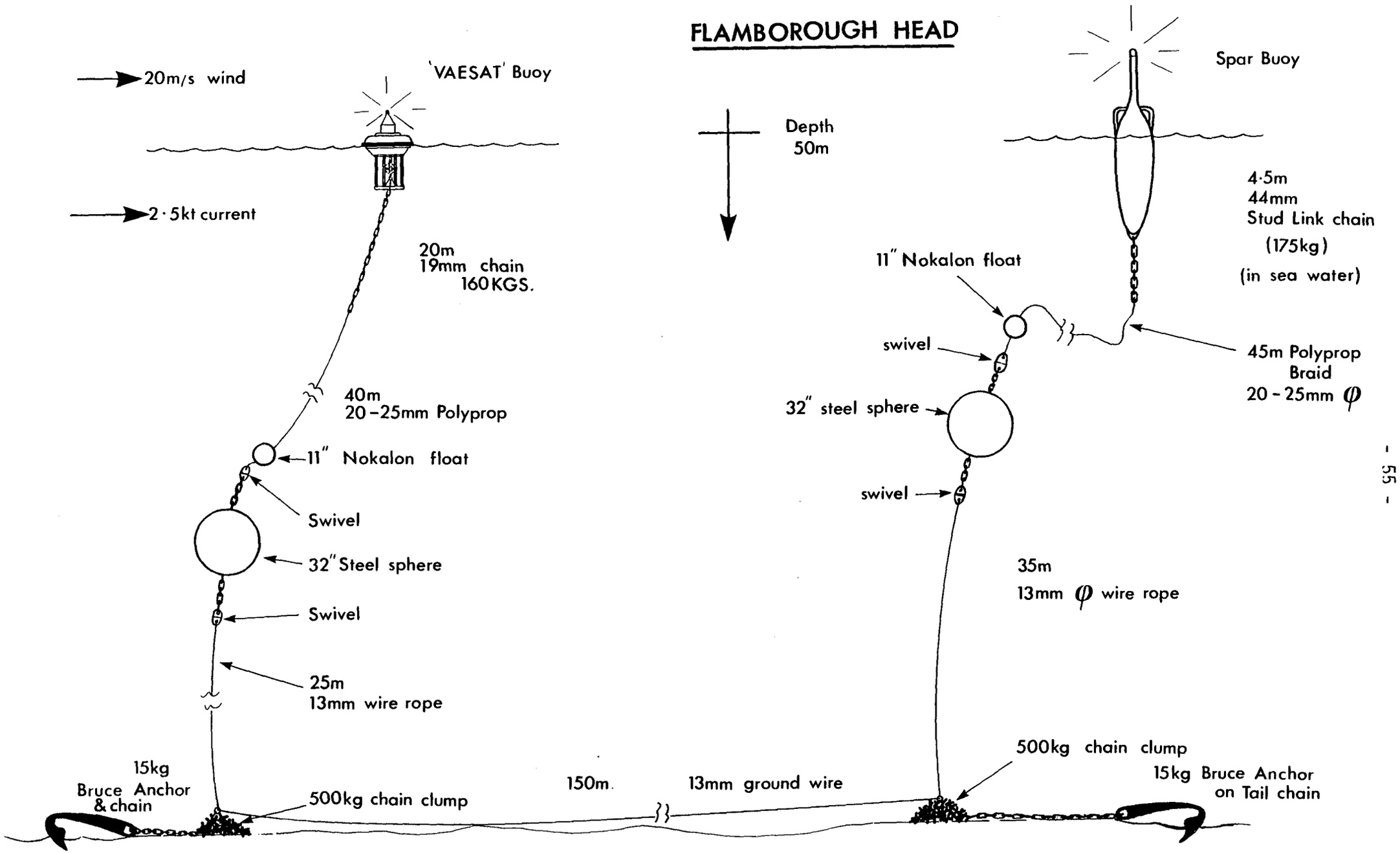

Figure 4.2 Flamborough current meter moorings.

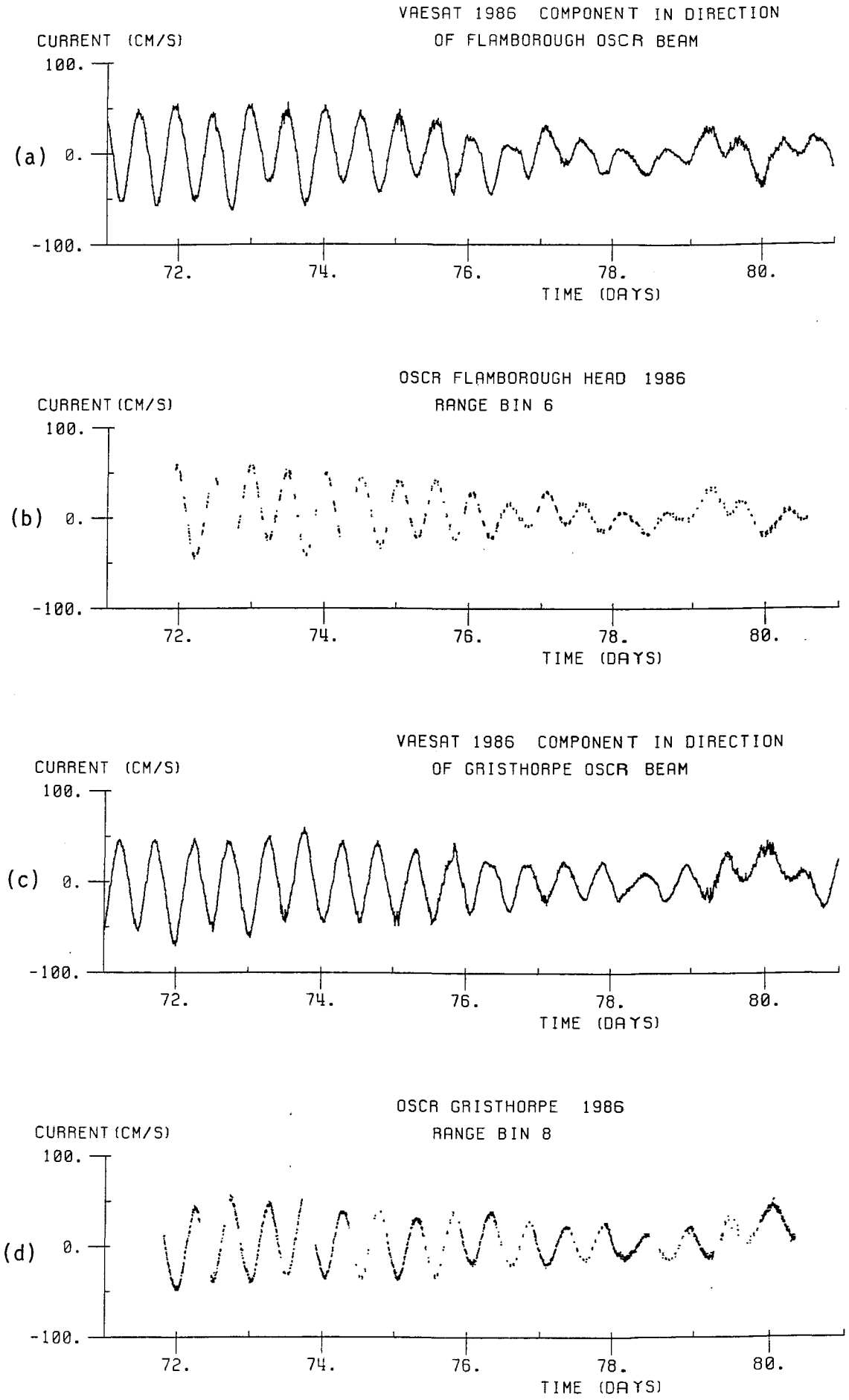

Figure 4.3 Time series of radial current components measured by surface buoy mounted instrument at 1 m (a), (c) and OSCR (b), (d).

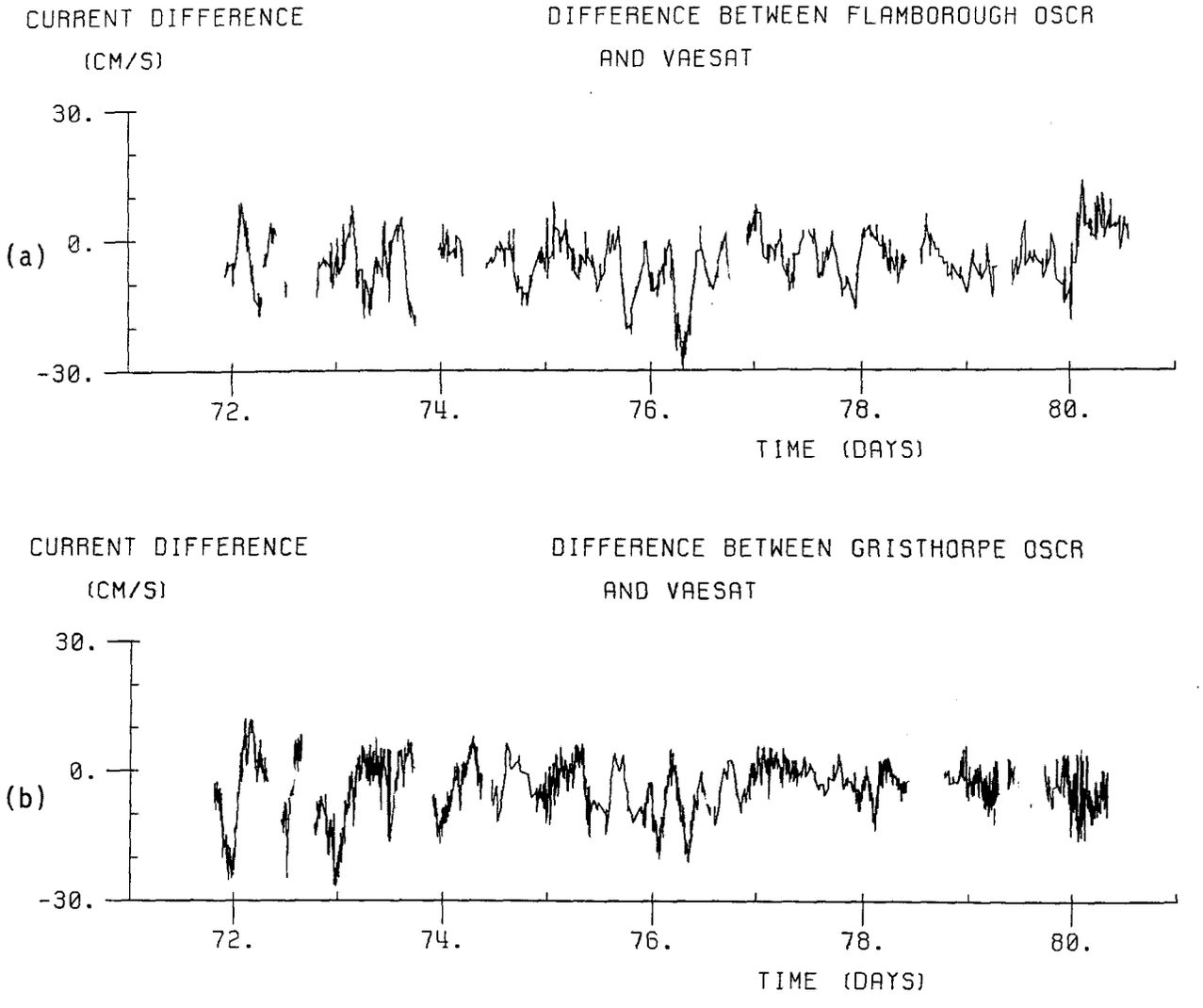

Figure 4.4 Differences in radial current components measured by OSCR and by the surface buoy mounted instrument at 1 m depth.
(a) Flamborough OSCR beam.
(b) Gristhorpe OSCR beam.

5. MEASUREMENT AND INTERPRETATION OF CURRENT PROFILES

The introduction to this report identified three areas of concern influencing wave-current interaction. One of these areas was the interaction of a wave field with a depth varying current. Current profiles near the sea surface, where the interaction would occur, are difficult to achieve using conventional instrumentation. To overcome the disadvantages of such instruments a slope-following buoy equipped with an electromagnetic current sensor at 1 m depth and an Acoustic Doppler Current Profiler (ADCP) were deployed as part of the instrumentation suite. The ADCP was moored beneath a spar buoy with the aim of making current measurements at ten levels from 19.9 m to 5.05 m depth.

Allied to the problem of making high quality current measurements in the near surface is the subsequent interpretation of the data. Several physical processes contribute to the total near-surface current and the relative importance of the processes may vary with location and season. It is important, therefore, to try and identify the sources of shear seen in the observations so that their relevance to other situations can be assessed.

5.1 South-West Approaches Current Meter Deployment

In order to achieve a high resolution in the vertical for the horizontal components of the current, two moorings were set near DB2 during Discovery Cruise 162. Mooring 413, shown in figure 5.1a, comprised a surface following VAESAT buoy as described by Collar et al. (1987) and a VACM. The mooring was laid with DB2 bearing 197° at a range of 0.7nm. Nearby, mooring 415, figure 5.1b, comprised a 10 m long spar buoy supporting three VAECMs (Clayson, 1983), a 1 MHz ADCP (Griffiths and Flatt, 1987) and an Aanderaa Pressure/Temperature logger. Details of the depths and sampling scheme are given in Table 5.1.

The primary instruments used to define the current profile were the VAESAT, VACM and the three VAECMs. Although the ADCP had previously been deployed on a bottom frame and on a sub-surface mooring, this was its first operational deployment beneath a spar buoy. As the ADCP relies on measuring the doppler shift of the backscatter from suspended matter in the water, the presence nearby of large discrete targets (the current meters and the spar buoy) posed a severe test of the sidelobe rejection of the acoustic

Instrument	Depth (m)	Record Start	Record End	Sampling Interval(s)	Parameters
VAECM10	31.1	211.46	246.69	56¼	VE,VN
VAECM2	29.6	210.83	234.51	56¼	VE,VN
VAECM1	14.9	210.83	225.50	56¼	VE,VN
VACM	4.0	210.45	246.80	450	VE,VN,T
VAESAT 2	1.0	210.45	246.80	60	VE,VN,T
ADCP	24.9(1)	210.96	247.67	720	VE,VN
AANDERAA(2)	35.9	210.83	250.00	600	T,P

Table 5.1 Details of the moored instruments deployed near DB2 for the wave-current interaction experiment. Time in Julian Days.
(1) The depth indicated was that of the ADCP transducers, current measurements were made at 1.65 m intervals between 19.9 m and 5.05 m.
(2) The Aanderaa current meter was stripped of its rotor and vane and used as a pressure/temperature logger.

transducers. Some contamination of the current record is believed to have occurred, especially at times of low scattering strength. Some solutions which may alleviate this problem are (i) to use a software based algorithm within the ADCP to identify and reject signal returns from hard targets, (ii) to use a sub-surface mooring with a strongly buoyant (>100 kg) ADCP tube as the uppermost part or (iii) to mount the ADCP within a surface following buoy.

5.2 **Data Analysis and Interpretation**

Table 5.2 shows the results of a tidal analysis of the current meter records for K1, the principal diurnal component, M2, the principal semi-diurnal component and M4, an indicator of non-linearity. The low east component at 1 m was the result of a faulty compass unit, we have assumed a correction factor of 1.8 for the data presented in the figures. The relatively low magnitudes of the M2 components at 15 m are not thought to be of instrumental origin, note that the K1 components are very similar to those at 20 m and 4 m. The mooring site was near the Celtic Sea shelf break where the barotropic M2 tide generates large internal tides as described by Pingree et al. (1984). This internal tide propagates on to the shelf and interacts non-linearly with the barotropic tidal

Depth (m)	K1E		K1N		M2E		M2N		M4E		M4N		MEAN	
	H	G	H	G	H	G	H	G	H	G	H	G	E	N
31.1	19	33.4	20	292.6	270	128.4	343	57.5	23	226.4	19	139.3	6	-42
19.6	29	40.6	29	318.4	301	130.1	358	60.6	24	157.4	27	85.1	58	-64
14.9	27	48.9	30	313.9	230	147.0	304	72.6	49	185.6	49	89.4	88	-98
4.0	26	40.7	31	285.4	296	148.2	401	73.3	21	238.4	32	136.9	42	-79
1.0	17	28.1	24	307.4	159	148.0	381	62.1	5	96.3	28	127.0	39	-61

Table 5.2 Tidal analysis for K1, M2 and M4. H is the magnitude in mm/s and G the phase in degrees with respect to the equilibrium tide. The record length analyzed was 29 days, except at 19.6 m and 14.9 m where the analysis was over 14 days.

currents. One indication of this non-linear behaviour is the mean residual current, noted in Table 5.2, predicted by the model of Pingree (1984) and observed by Maze (1987) some 160 km to the south east of our moorings. The mean current within the mixed layer for the first 14 days of our deployment was 94 mm/s directed at 143°, close to the local shelf edge orientation of 120°. Another indicator of the presence of an internal tide is an anomalous value for the M4 component. Table 5.2 shows that the M4 components, as well as the mean flow, reach a peak at a depth of 15 m, where the M2 components were a minimum. This non-linear interaction of the barotropic and internal tide produced a shear of about 0.011 s^{-1} at the M2 tidal frequency between 15 m and 4 m.

5.3 Sub-tidal currents

Two significant storms occurred during the overlap period of the current meter array and DB2. The mean wind speed during the first storm on day 213 reached 19 m/s and the second storm persisted from day 217 to 219 with comparable wind speeds. Both storms produced distinct events in the low-pass filtered current. A Lanczos squared digital filter with a cut-off period of 25 hours was applied to the time series of the current meters and the resulting current magnitudes are shown in the form of a contour plot in figure 5.2. Prior to the storm the mixed layer depth (MLD) was between 10 and 20 m (the range being due to the modulation of the MLD by internal waves). During the build-up of the wind driven current three regions were present:

(i) the current at 1 m responded quickly to the increasing wind speed and reached a higher peak than the current at 4 m,

(ii) the current between 4 m and 20 m (approximately the initial MLD) responded uniformly,

(iii) at 31 m the current increased after an initial lag (more clearly seen in figure 5.6) and reached a lower peak value.

The record from the P/T logger showed that by the end of the storm the MLD was approaching 35 m. Note that the shear implied in figure 5.2 between 30 m and 20 m was less during the decrease in wind speed after the height of the storm than during its build up. This leads to the conclusion that the strongest shear existed near the base of the mixed layer, or across the thermocline. Such an assumption is consistent with the so-called 'slab models' of mixed layer flow (see Gordon (1982) for a review of such models).

Figure 5.3 shows in vector form the wind and low pass filtered currents during the first storm. The current at 1 m was deflected to the right of the wind, the deflection decreasing from ~45° to ~22° as the wind speed increased. A substantial shift in direction developed between 1 m and 4 m during the build up of the storm, with the layer between 4 m and 20 m showing more uniform flow. Note the change in magnitude and direction between 20 m and 30 m as the thermocline was approached.

5.4 The Nature of the Near-Surface Current

The interpretation of the near-surface current is complex largely due to the multitude of physical processes contributing to the total current. Further, the interactions between these physical processes and the methods of instrument deployment add to the difficulties. Practical current measurement methods fall between the two ideal frames of reference, Eulerian and Lagrangian:

(a) a true Eulerian measurement would require a rigidly fixed current sensor, in many situations this is a practical impossibility and is usually approximated by a taut sub-surface mooring or by suspension under a spar buoy;
(b) a true Lagrangian measurement requires the tracking of water particle trajectories and the conversion of position changes to velocity, an example of a practical method being acoustically tracked floats.

Whereas the VAECMs and the ADCP mounted beneath the spar buoy approximate an Eulerian frame of reference the slope-following VAESAT buoy attempts to follow the surface orbital motion of the gravity waves. Hence it may be considered to be quasi-Lagrangian. This distinction between the frames of reference is important if accurate conclusions are to be drawn about the nature of the near-surface current profile. An important difference between the two frames of reference lies in their treatment of Stokes Drift - a current arising out of the change in orbital velocity with depth, the forward velocity at the crest of a wave being larger than the backward velocity at the trough produces a net wave-related current which decays rapidly with depth. Whereas the Stokes Drift is included in the current measured in a Lagrangian frame of reference, it is not measured by an Eulerian sensor. Collar et al. (1983), in an analysis of

the response of a current sensor mounted rigidly beneath a slope-following buoy in monochromatic waves, showed that such an instrument would include in its measurement a component approximating the surface value of the Stokes Drift.

As yet, a consensus has not been reached on the role of Stokes Drift in the open sea. Recent theoretical work by Jenkins (1987) postulates a ratio of about 3:1 between the Lagrangian and quasi-Eulerian components of the surface current, however, no observations in support of this ratio were given. We believe that the distinction between Eulerian and Lagrangian residual flow and their (probably) separate evolution and decay is important to the study of current shear in the upper ocean.

5.4.1 A Simple Geometrical Model of the Current Components at 1 m

In an attempt to show qualitatively the independent behaviour of the purely Eulerian component and the Stokes Drift component of the current at 1 m, as measured by the VAESAT buoy, we construct a simple geometrical model. Henceforth in this section Lagrangian will be taken to mean that component of the total flow not measured by an Eulerian sensor.

If we make the following assumptions about the nature of the currents at 1 m and 4 m shown in figure 5.4:

(i) Eulerian current at 1 m to be not less than that at 4 m (curve A),
(ii) deflection angle of both Lagrangian and Eulerian components at 1 m to be less than or equal to the Eulerian deflection at 4 m (line B),
(iii) minimum deflection of Lagrangian component at 1 m to be along the vector joining the endpoints of the 4 m and 1 m currents (line C),

then the relationship between the Eulerian and Lagrangian components in the

following areas can be determined:

Area bounded by:

ABC — Endpoint of the Eulerian current vector at 1 m drawn from the origin can lie in this region. The remaining vector to D being the Lagrangian component. This area can be subdivided into:

(i) AEC — If the Eulerian current vector endpoint lies in this area then the Lagrangian deflection is to the left of the wind.

(ii) AEF — In this area the deflection to the right of the Lagrangian component is less than that of the Eulerian component.

(iii) AFB — In this area the deflection to the right of the Lagrangian component is greater than that of the Eulerian component.

If we assume the theoretical results of Jenkins (1987) which suggest a Lagrangian deflection to the right, though less than the Eulerian deflection, then areas AEC and AFB can be neglected. Therefore the likely endpoint of the Eulerian vector must lie within the area AEF. Figure 5.5 shows this procedure applied to the data during the first storm. The possible area for the Eulerian component endpoint increases during the first 8 hours of the storm, then it decreases to virtually zero at 16 hours before going negative at 20 hours (the negative area may be due to the correction factor used in the 1 m east component due to the compass error). This reduction in area raises the possibility of a Lagrangian current which decreases to zero and becomes an Eulerian oscillation on a timescale comparable to an inertial period, as suggested by Ursell (1950). However, because the Eulerian current vector could end anywhere within AEF, including point D, no certain conclusions regarding the Lagrangian current can be drawn.

5.5 Storm Driven Continental Shelf Waves

Gordon and Huthnance (1987) state that continental shelf wave (CSW) dynamics dominate the ocean response to storm forcing over continental shelves near the shelf break. They found an oscillatory response with a frequency of about 0.6f (f being the local inertial frequency) on the Scottish shelf east and west of the Shetlands. The present data set was examined for evidence of CSWs.

Figure 5.6 shows the low pass filtered current magnitude during the first storm as a percentage of wind speed, with wind speed shown for reference. The substantially higher current at 1 m and the lag at 30 m are clearly seen. What is also clear is that the wind driven current, in percentage terms, started to decrease before the wind speed reached a maximum. Later, as the wind speed decreased the percentage current increased, first at 1 m then at the other depths. The period of this fluctuation was approximately 24 hours or 0.54f, similar to the observations of Gordon and Huthnance (1987).

The rise in percentage current around day 214.5 shown in figure 5.6 is also shown in the contour plot, figure 5.2, although it is not so obvious. However, around day 215.25 figure 5.2 shows a strong current confined to the centre of the mixed layer which was not associated with the wind. This peak occurred about 16 hours, or an inertial period, after the previous peak. The persistence of CSWs and inertial oscillations after the passage of a storm add to the complexities of near-surface flow. Indeed, the baroclinic oscillation around day 215.25 showed a greater shear ($0.009s^{-1}$) between 15 m and 4 m in calm weather ($<5ms^{-1}$) than during the height of the storm ($<0.0015s^{-1}$).

5.6 Conclusions regarding the Current Profile

The current meters deployed on the two moorings near DB2 provided a high resolution in the vertical for the measurement of horizontal current and current shear. Analysis of the data yielded the following conclusions:

(i) The non-linear interaction of the barotropic M2 tide with the internal tide generated at the shelf break resulted in an along shelf residual current and anomalous values of the M4 component. This interaction was the possible cause of a shear of $0.011s^{-1}$ in the M2 tidal current between 15 m and 4 m.

(ii) During the first storm the Eulerian currents at depths of 4 m and greater within the mixed layer were virtually uniform (shear $<0.0015s^{-1}$).

(iii) Stronger shear ($\sim 0.010s^{-1}$) existed near the base of the mixed layer which deepened during the passage of the storm.

(iv) The near-surface response, as defined by the measurements at 1 m and 4 m, was dominated by the contribution, if any, of a Lagrangian current to the 1 m measurement. Using a few basic assumptions the set of possible Eulerian/Lagrangian vectors was delineated. Until a like-with-like comparison can be achieved in the upper 5 m great caution should be taken in interpreting the apparent shear.

(v) The after-response of the continental shelf to storm winds as exemplified by CSWs and inertial oscillations, for which some evidence has been seen in our data, complicate the interpretation of the current profile. These low frequency events produced greater shear ($\sim 0.009s^{-1}$) than the storm which generated them.

(vi) Mooring an ADCP beneath a spar buoy, which also supported other current meters, gave rise to problems due to reflections from the discrete targets. A taut sub-surface mooring would be preferable. An alternative approach would be to mount the ADCP within the VAESAT buoy, looking downwards. Such an arrangement would provide a like-with-like comparison with the VAESAT 1 m current measurement. This facility is being developed at IOSDL.

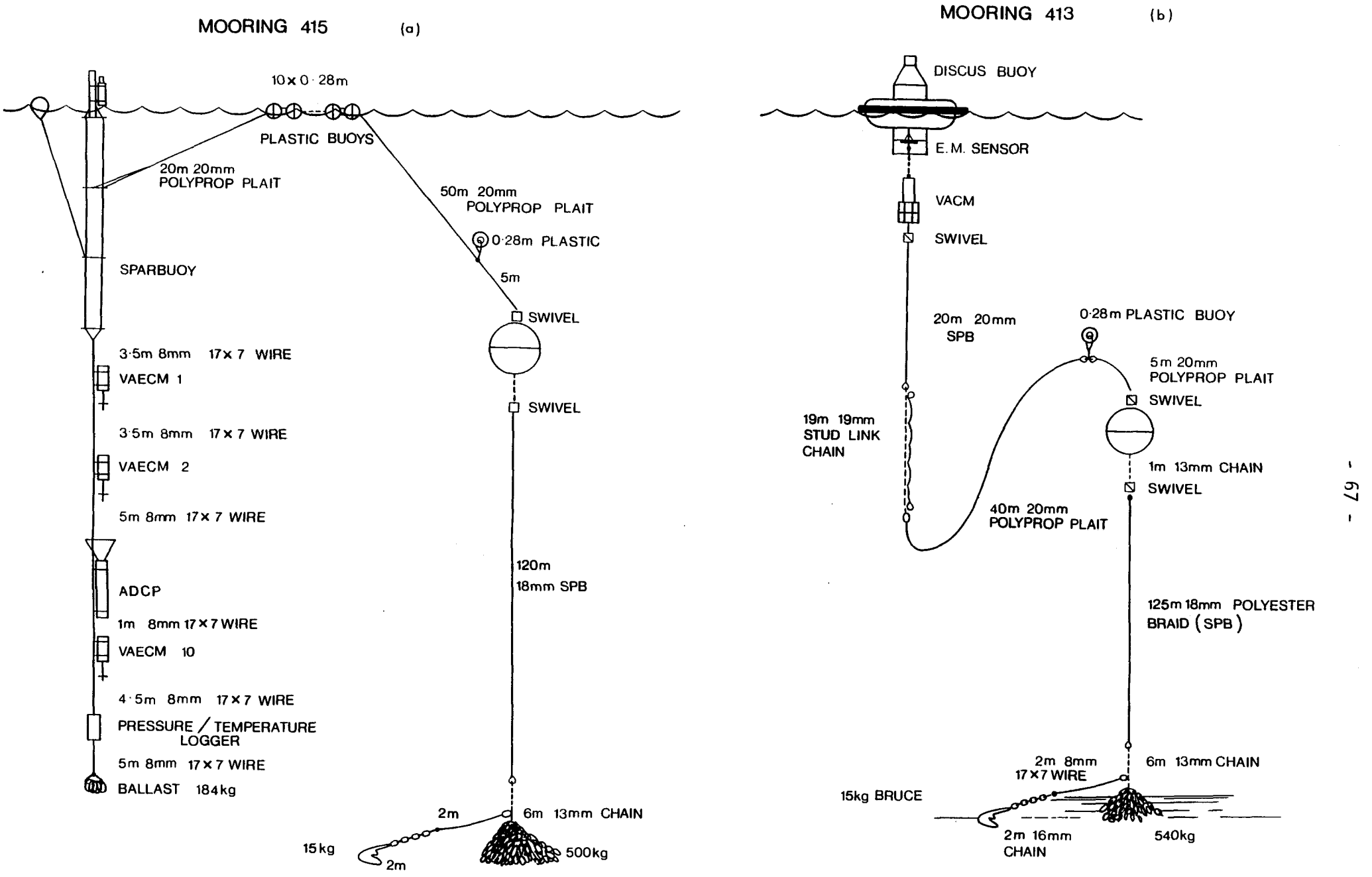

Figure 5.1 Arrangement of instruments on the two moorings deployed near DB2 for the wave/current interaction study.

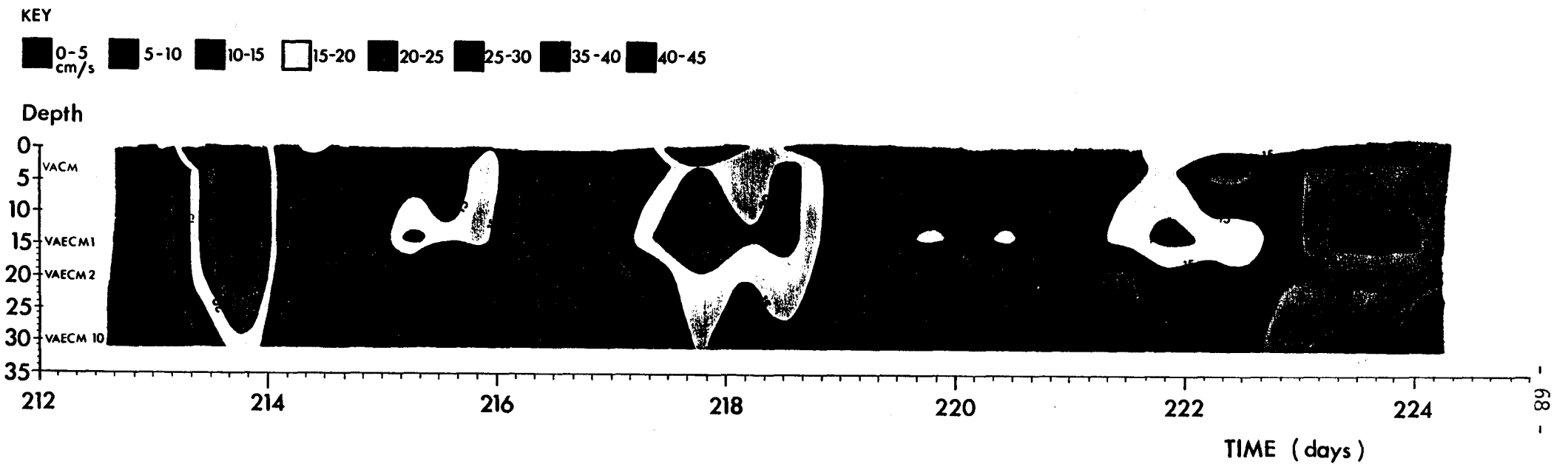

Figure 5.2 Contour plot of the low pass filtered current magnitudes.

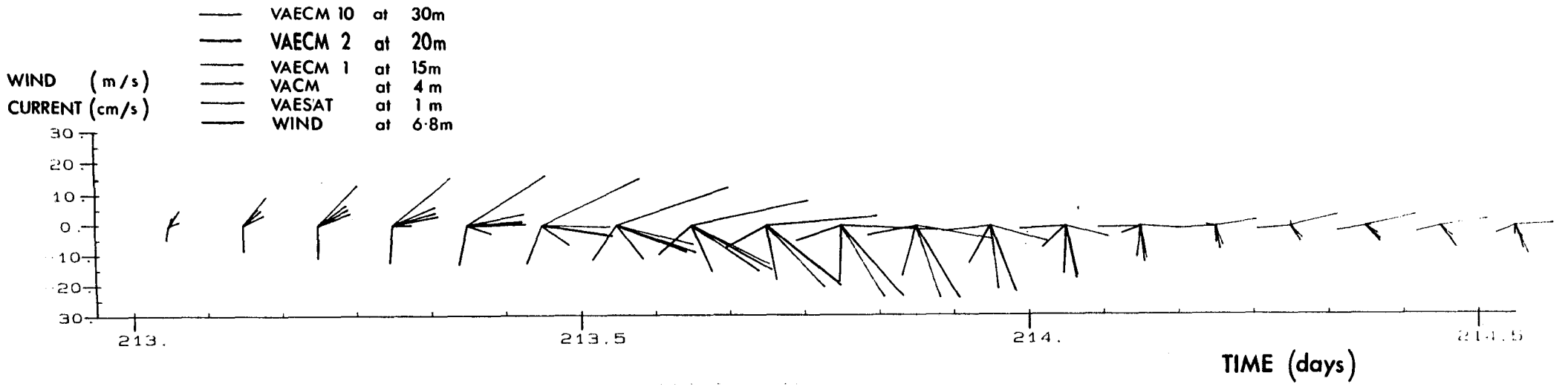

Figure 5.3 Vector plot of the wind and currents during the first storm

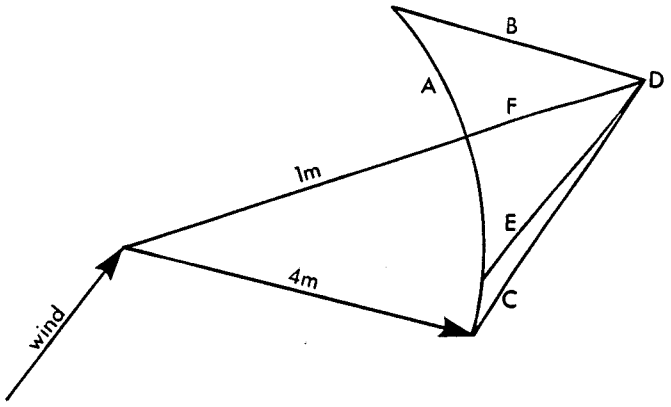

Figure 5.4 Geometrical construction showing the areas of possible Eulerian/Lagrangian vector endpoints.

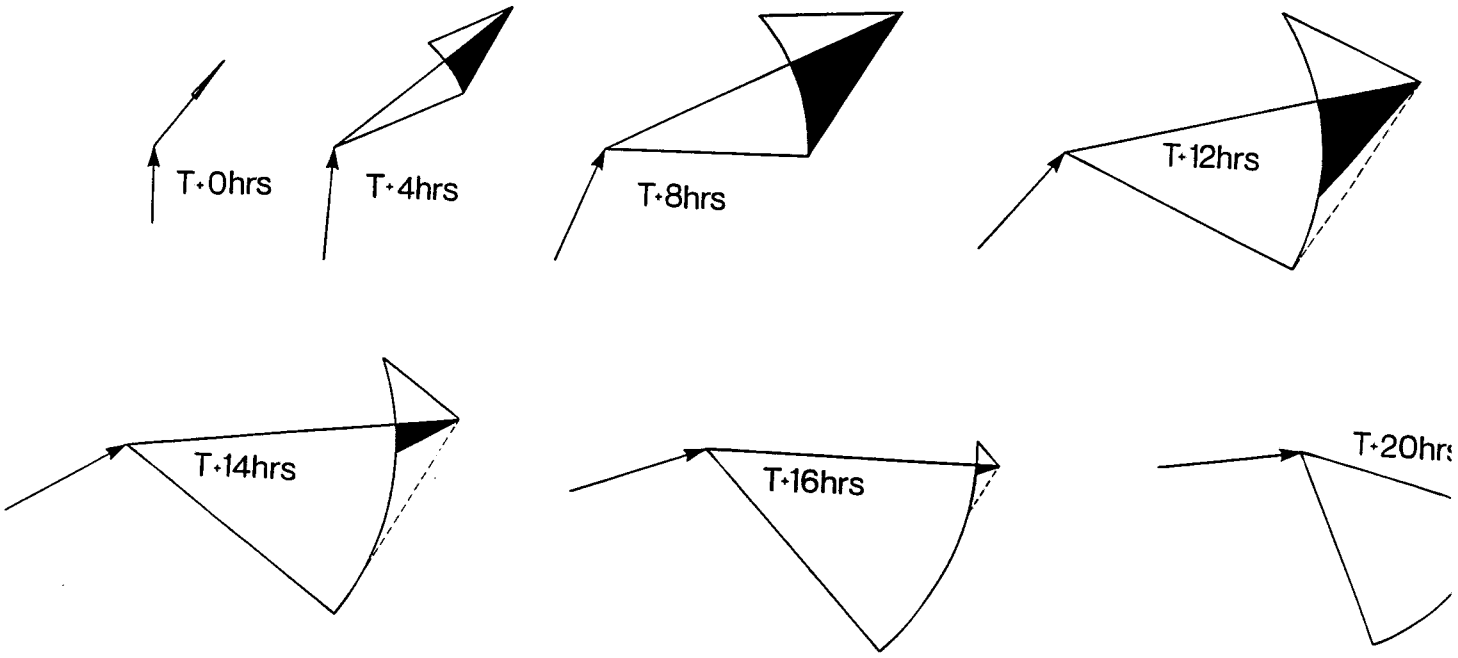

Figure 5.5 Areas of possible Eulerian/Lagrangian vector endpoints during the first storm.

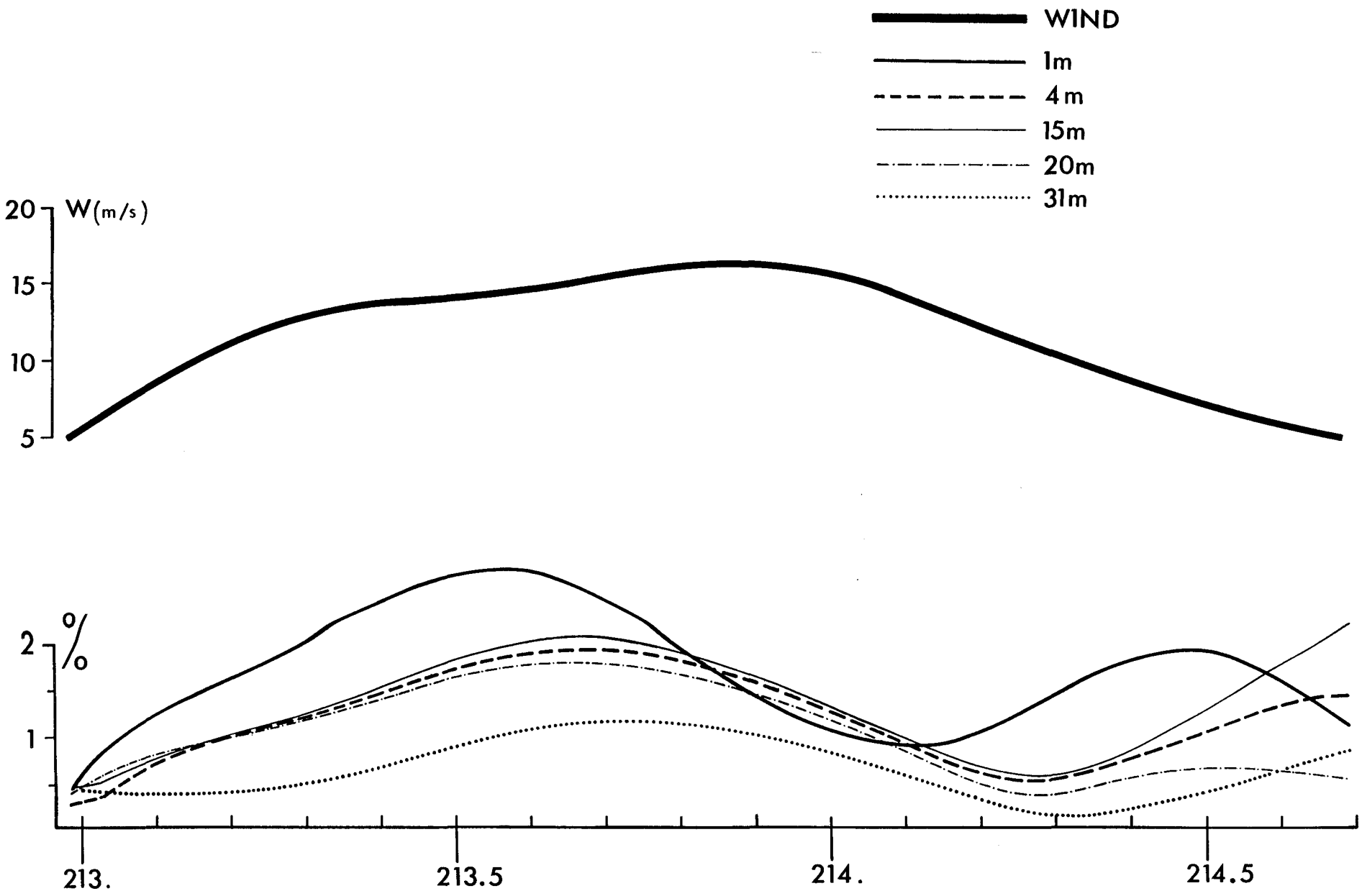

Figure 5.6 Low pass filtered current magnitude during the first storm expressed as a percentage of wind speed with wind speed shown for reference.

REFERENCES

BRETHERTON, F.P. & GARRETT, C.J.R. 1968 Wavetrains in inhomogeneous moving media.
Proceedings of the Royal Society, A 302, 529-554.

CLAYSON, C.H. 1983 A Vector Averaging Electromagnetic Current Meter for near-surface measurement.
pp. 81-87 in, Proceedings 1983 Working Symposium on Oceanographic Data Systems, WHOI, 4-6 October 1983 (ed. C.D. Tollios, M.K. McElroy & J. Syck) Silver Spring, MD: IEEE Computer Society Press/WHOI, 199pp.

COLLAR, P.G., CARSON R.M. & GRIFFITHS, G. 1983 Measurement of near-surface current from a moored wave-slope follower.
Deep-Sea Research, 30, 1, 63-75.

COLLAR, P.G., HUNTER, C.A., PERRETT, J.R. & BRAITHWAITE, A.C. 1987 Measurement of near-surface currents using a satellite telemetering buoy.
pp. 49-56 in, Fifth International Conference on Electronics for Ocean Technology, Edinburgh, 24-26 March 1987.
London: Institution of Electronic and Radio Engineers, 223pp.
(IERE Publication No. 72).

COLLAR, P.G. & HOWARTH, M.J. 1987 A comparison of three methods of measuring surface currents in the sea: radar, current meters and surface drifters.
D.En. Offshore Technology Report, OTH 87272.

CRAPPER, G.D. 1984 Introduction to Water Waves.
Chichester: Ellis Harwood Ltd., 224pp.

EASTWOOD, J.W., TOWNEND, I.H. & WATSON, C.J.H. 1987
pp. 327-342 in, Advances in Underwater Technology, Ocean Sciences and Offshore Engineering, Volume 12, Modelling the Offshore Environment.
London: Graham and Trotman.

GONZALEZ, F.I. 1984 A Case Study of Wave-Current Bathymetry Interactions at the Columbia River Entrance.
Journal of Physical Oceanography, 14, 1065-1078.

GORDON, R.L. 1982 Coastal Ocean Current Response to Storm Winds.
Journal of Geophysical Research, 87, C3, 1939-1951.

GORDON, R.L. & HUTHNANCE, J.M. 1987 Storm-driven continental shelf waves over the Scottish continental shelf.
Continental Shelf Research, 7, 9, 1015, 1048.

GRIFFITHS, G. & FLATT, D. 1987 A self-contained acoustic Doppler current profiler - design and operation.
pp. 41-47 in, Fifth International Conference on Electronics for Ocean Technology, Edinburgh, 24-26 March 1987.
London: Institution for Electronic and Radio Engineers, 223pp.
(IERE Publication No. 72).

HUANG, N.E. 1971 Derivation of Stokes drift for a deep water random gravity wave field.
Deep-Sea Research, 18, 255-259.

HUANG, N.E., CHEN, D.T. & TUNG., C. 1972 Interactions between steady non-uniform currents and gravity waves with applications for current measurements.
Journal of Physical Oceanography, 2, 420-431.

JENKINS, A.D. 1987 Wind and wave induced currents in a rotating sea with depth varying eddy viscosity.
Journal of Physical Oceanography, 17, 938-951.

LAMBROKES, K.F. 1981 Wave-current interaction effects on water velocity and surface wave spectra.
Journal of Geophysical Research, 86, C11, 10955-10960.

LONGUET-HIGGINS, M.S., CARTWRIGHT, D.E. & SMITH, N.D. 1963 Observations of the directional spectrum of sea waves using the motions of a floating buoy.
pp. 111-136 in, Ocean Wave Spectra.
Englewood Cliffs: Prentice-Hall.

LONGUET-HIGGINS, M.S. & STEWART, R.W. 1964 Radiation stress in water waves; a physical discussion with applications.
Deep-Sea Research, 11, 529-562.

MAZE, R. 1987 Generation and propagation of non-linear internal waves induced by the tide over a continental slope.
Continental Shelf Research, 7, 9, 1079-1104.

PEREGRINE, D.H. 1976 Interaction of Water Waves and Currents.
Advances in Applied Mechanics, 16, 9-117.

PEREGRINE, D.H. & JONSSON, I.G. 1983 Interactions of waves and currents.
U.S. Army, Corps of Engineers, Coastal Engineering Research Center, Miscellaneous Report, No. 83-6, 88pp.

PINGREE, R.D., GRIFFITHS, D.K. & MARDELL, G.T. 1984 The structure of the internal tide at the Celtic Sea shelf break.
Journal of the Marine Biological Association of the United Kingdom, 64, 99-113.

PITT, E.G., PASCAL, R.W. & VAN HETEREN, J. 1985 A comparison of the measurements made by two pitch-roll buoys during the NURWEC project.
pp. 247-267 in, Advances in Underwater Technology and Offshore Engineering, Vol. 4, Evaluation, Comparison and Calibration of Oceanographic Instruments.
London: Graham and Trotman.

SHEARMAN, E.D.R. 1981 Area surveillance of sea state, surface current and surface wind by dekametric radar technique.
pp. 101-112 in, Proc. IERE Conference Electronics for Ocean Technology, Birmingham, September 1981.

SROKOSZ, M.A. 1987 Models of Wave-Current Interaction.
pp. 313-325 in, Advances in Underwater Technology, Ocean Science and Offshore Engineering, Vol. 12, Modelling the Offshore Environment. London: Graham and Trotman.

URSELL, F. 1950 On the theoretical form of ocean swell on a rotating earth. Monthly Notices of the Astronomical Society, Geophysical Supplement, 6, 1-8.